The amalgamation of Gondwana: calcite twinning and finite strains from the early-late Paleozoic Buzios, Ross, Kurgiakh and Gondwanide orogens

John Craddock[1]*, Timothy Paulsen2, Renata da Silva Schmitt\ Stephen T. Johnston4, Paul M. Myrow[5] and Nigel C. Hughes[6]

[1]Geology Department, Macalester College, 166 Macalester Street, St Paul, MN 55105, USA

[2]Departrnent of Geology, University of Wisconsin Oshkosh, 845 Elmwood Avenue, Oshkosh, WI 54901, USA

[3]Departrnent of Geology, Institute of Geosciences, Universidade Federaldo Rio de Janeiro, llha do Fundao, Rio de Janeiro, Brazil

[4]Departrnent of Earth and Atmospheric Sciences, University of Alberta, 1-26 Earth Sciences Building, Edmonton, Alberta, Canada T6G 2E3

[5]Colorado College, Palmer Hall #9E, Colorado Springs, CO 80946, USA

[6]Departrnent of Earth and Planetary Sciences, University of California, Riverside, 900 University Avenue, CA 92521, USA

G JC, 0000-0002-4478-7672

*Correspondence: craddock.irnp@gmail.com

Abstract: Orientatedcatbonate(calcite twinning strains;n =78 with 2414 twin measurements) and quartzites (finite strains;n = 15) werecollected around Gondwana to study the deformational history associated with the amalgamation of the supercontinent The Buzios orogen (545-500 Ma), within interior Gondwana, records the high-grade collisional orogen between the Sao Francisco Craton (Brazil) and the Congo-Angola Craton (Angola and Namibia), and twinning strains in calc-silicates record a SE-NW shortening fabric parallel to the thrust transport Along Gondwana's southern margin, the Saldanian-Ross-Delamerian orogen (590-480Ma)is marked by a regional unconformity that cutsintodeformed Neoproterozoic-Ordoviciansedimentary rocks and associated intrusions. Cambrian carbonate is preserved in the central partof the southern Gondwana margin, namely in the Kango Inlier of the Cape Fold Belt and the Ellsworth, Pensacola and Transantarctic mountains. Paleozoic catbonate is not preserved in the Ventana Mountains in Argentina, in the Falkland Islands/Islas Malvinas or in Tasmania. Twinning strains in these Cambrian catbonate strata and synorogenic veins record a complex, overprinteddeformation history with no stableforeland strain reference. The Kurgiakh orogen (490Ma) along Gondwana's northern margin is also defined by a regional Ordovician unconformity throughout the Himalaya; these rocks record a mix of layer-parallel and layer-normal twinning strains with a likely Himalayan (40 Ma) strain overprint and no autochthonous foreland strain site.

Conversely, the Gondwanide orogen (250 Ma) along Gondwana's southern margin has three foreland (autochthonous) sites for comparison with 59 allochthonous thrust-belt strain analyses. From west to east, these include: finite strains from Devonian quartzite preserve a layer-parallel shortening (LPS) strain rotated clockwise in the Ventana Mountains of Argentina; frontal (calcite twins) and internal (quartzite strains)samples in the Cape Fold Belt preserve a LPS fabric that is rotated clockwise from the autochthonous north-south horizontal shortening in the foreland strain site; Falkland Devonian quartzite shows the same clockwise rotation of the LPS fabric;and Permian limestone and veinsin Tasmania record a thrust transport-parallel LPS fabric.Early amalgamation of Gondwana (Ordovician) is preserved by local layer-parallel and layer-normal strain without evidence of far-field deformation, whereas the Gondwanide orogen (Permian) is dominated by layer-parallel shortening, locally rotated by dextral shear along the margin, that propagated across the supercontinent.

The *c*. 700-500 Ma assembly of Gondwana was a protracted process that involved the Pan-African collision of cratons in the interior of Gondwana, as well as accretionary orogenesis along its margins (Cawood 2005; Cawood and Buchan 2007; Nelson and Tuttle 2018; Schmitt *et al.* 2018; Cawood *et al.* 2021). In many areas, these late Neoproterozoic-Ordovician orogenic beltsexperienced extensiveerosion, creating peneplains on which regional transgressive sandstones, glacial deposits (Craddock *et al.* 2019b) and *Glossopteris-bearing* shale were subsequently deposited (du Toit 1937). In the late Paleozoic, some of these sedimentary successions were involved in shortening associated with the

From: Hynes, A. J. and Murphy, J.B. (eds) *TheConsummate Geoscientist: A Celebration of the Career of Maarten de Wit.* Geological Society, London, Special Publications, 531,
https://doi.org/l0.1144/SP53l-2022-l65

Gondwanide orogen (Craddock 1982; Halbich and Swart 1983; de Wit 1992; Dalziel 1997), and a thin-skinned belt formed along the continent's trailing southern margin of Gondwana as it collided to the north with Laurentia (Appalachian-Caledonide-Variscan belt: Cawood and Buchan 2007; Craddock *et al.* 2017c) during the assembly of Pangaea. Although these orogenic episodes have long been known, there is a general lack of strain data despite their potential to provide valuable information about the geodynamic processes involved in super-continent assembly. We provide strain data from these early and late Paleozoic orogenic belts found around Gondwana (Argentina, Brazil, southern Africa, theFalklandIslands/Islas Malvenas, theEllsworth and Transantarctic Mountains, Tasmania, and the Himalaya: Figs l-5) and compare the strain fields that propagated across Pangaea through these two orogenic cycles (Wilson 1966; Veevers *et al.* 1997) in order to assess the kinematic dynamics and responses to the assembly of Gondwana.

Regional geology

Reconstructions of the Rodinia supercontinent are constrained by palaeopole data, and the realignment of the Grenville orogen (*c.* 1200-980 Ma) belts through North and South America, Antarctica, southern Africa, and India (Powell *etal.* 1993; Li andPowell 2001; Meert and Powell 200I; Meert 2003; Meert and Torsvik 2003; Torsvik 2003; Tohver *etal.* 2006; Goodge *et al.* 2010; Loewy *et al.* 2011; Torsvik and Robin Cocks 2013; Craddock *et al.* 2017a; Palin *et al.* 2018). The break-up of Rodinia (*c.* 800-700Ma) set the stage for the protracted assembly of Gondwana. Tectonomagmatic events are recorded in Neoproterozoic-lower Paleozoic mobile belts that wrapped around Precambrian cratonic cores, including the Pan-African orogen (*c.* 650-550 Ma), as well as Neoproterozoic--early Paleozoic mobile belts that formed along the supercontinent's margins (Boger and Miller 2004; Boger 2011). During the Cambrian-Ordovician, the peri-Gondwana realm was characterized by the deposition of siliciclastic sediment and minor carbonate. Examples include the Cambrian Kango Group exposed in a structural window in the central Cape Fold Belt (Barnett *et al.* 1997; de Wit *et al.* 1998), the Cambrian-Ordovician Heritage Group section in the southern Ellsworth Mountains, Antarctica (Webers *et al.* 1992), the Cambrian-Ordovician Byrd Group and Liv Group exposed along the length (1300 km) of the Transantarctic Mountains (Stump 1992, 1995; Myrow *et al.*

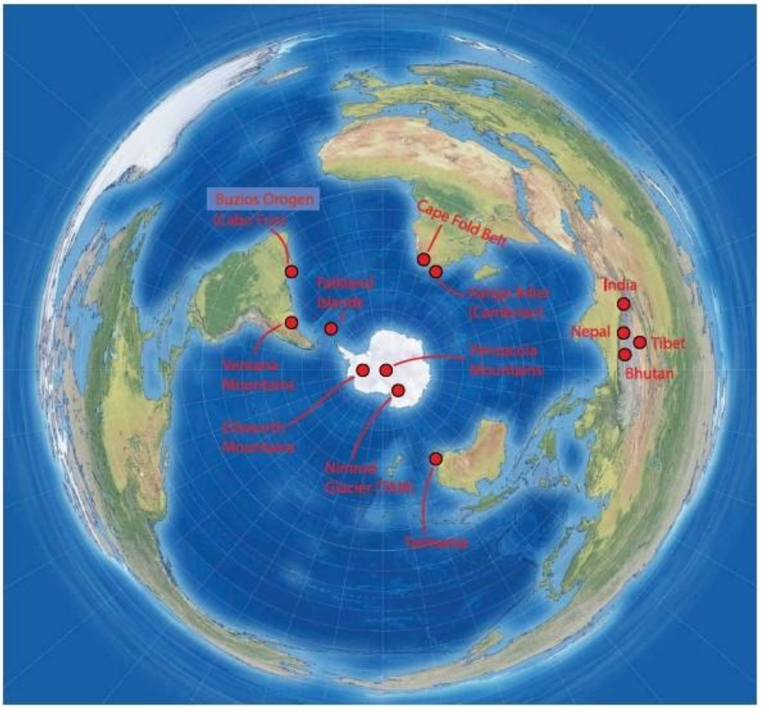

Fig. 1. South polar projection indicating the field locations for strain data (fables I & 2) of now widely separated portionsof Gondwana. **TAM,** Transantarctic Mountains.

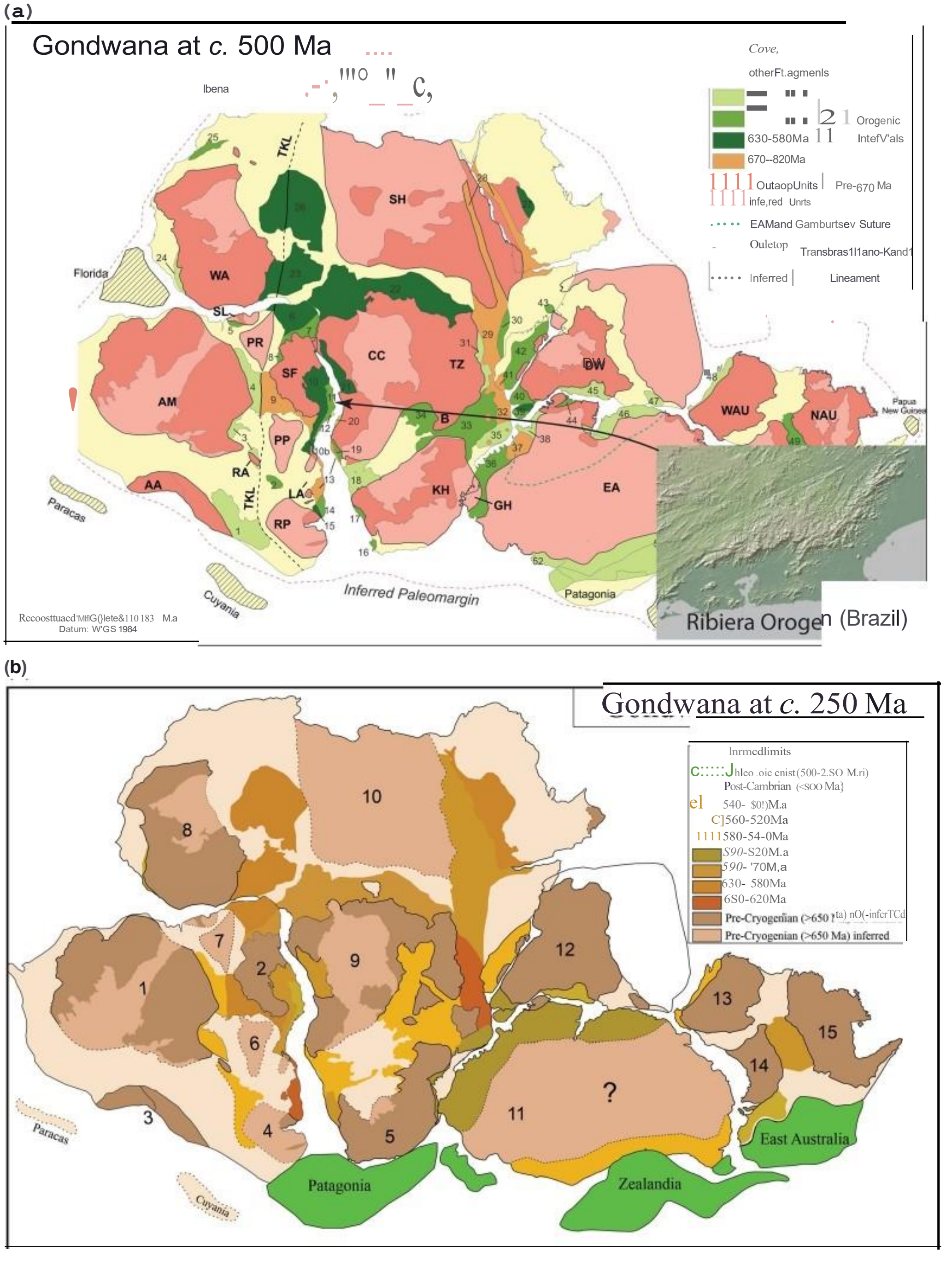

Fig. 2. Gondwana reconstructions at the end-Proterozoic (a: Terra Ausiralia orogen) and the late Paleozoic **(b:** Gondwanide orogen); see Figure I) for the locations of field sites and strain data (Tables I & 2).

2002; Goodge 2020), and Cambrian sedimentary sequences found along the Himalaya (Myrow *et al.* 2016). In some cases, these Cambrian successions lie on angular unconformities developed during earlier phases of deformation and exhumation (e.g. the Pensacola Mountains: Curtis *et al.* 2004).

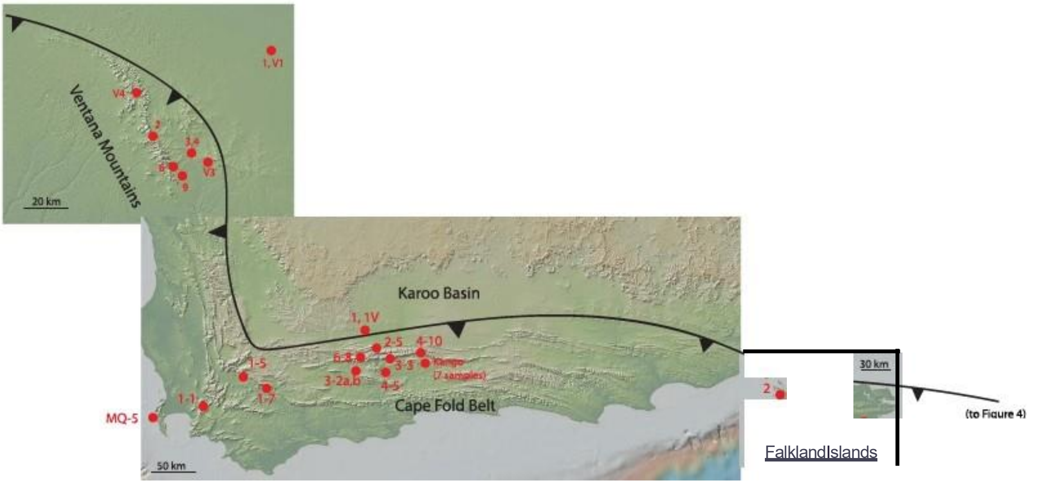

Fig. 3. DEM base (GeoApp 3.6.6) of the western part of the Gondwanide belt with sample sites identified. See Tables I & 2.

Deformation of these Cambrian-Ordovician sections have a plethora of local orogen names and tectonic belts (Cawood and Buchan 2007). In the interior of Gondwana, the collision of the Sao Francisco Craton (Brazil) and Congo-Angola Craton (Angola and Namibia), at 540-490 Ma, is known as the Buzios orogen (Schmitt *et al.* 2004, 2012, 2018), and created calc-silicates ideal for calcite strain analysis. Along Gondwana's southern margin, theRossorogen includes deformed Cambrian-Ordovician sedimentary rocksexposed along theTransantarctic Mountains, here these rocks are typically metamorphosed togreenschist to amphibolite facies, are gently to tightly folded, are characterized by a weak to pervasive local cleavage, are intruded by *c.* 500 Ma granitoids and rest unconformably below Devonian sandstone at the baseof the Beacon Supergroup (Stump 1992, 1995; Elliot 2013; Goodge 2020). Deformation and magmatism contemporaneous with that of the Ross orogen extends to areas in South America and Australia, and is likely to include the mild deformation found in the lower Paleozoic section of the Pensacola and Ellsworth mountains, and in the Kango Inlier carbonate of southern Africa (Craddock 1982; Stump 1995; Encamaci6n and Grunow 1996; Curtis 1998; de Wit *et al.* 1998; Duebendorferand Rees 1998; Foster *et al.* 2005; Foden *et al.*2006; Gonzalez *et al.* 2018; Goodge 2020). Along Gondwana's northern margin, the Kurgiakh Orogeny is recorded in the Tethyan Himalaya by local folds and faults, low grade (diagenetic to low epizone) to higher grade (garnet) *c.* 490 Ma metamorphism, 552-479 Ma granitic intrusions, and an unconformity that is locally angular and which is overlain by Ordovician conglomerate. The latter is also expressed in the Lhasa and Qiantang terranes of Tibet and in the Baoshan Blockof western Yunnan (DeCelles *et al.* 2000;Miller *et al.*2001; Myrow *et al.* 2003, 2016; Gehrels *et al.* 2006; Cawood *et al.* 2007; Torsvik *et al.* 2009). Along the northern margin of West Gondwana, the Cadomian-Avalonian orogen primarily records active margin volcanism and sedimentation from *c.* 800 to 530 Ma. Subsequent Cambrian volcanism and sedimentation has been attributed to lithospheric extension, although some authors suggest that the Cambrian-Ordovician magmatism locally occurred in association with an episode of crustal thickening that extended until *c.* 480 Ma, followed by post-orogenic deposition of Ordovician siliciclastic sediments along a passive margin (Villaseca *et al.* 2016; Garcia-Arias *et al.* 2018; Cawood *et al.* 2021).

After early Paleozoic deformation, Ordovician-Carboniferous age strata were deposited along the northern Gondwana passive margin in India, followed by emplacement of the lower Permian Panjal Traps, and associated rifting and formation of the Neo-Tethys Ocean (Draganits *et al.* 2005). Post-rift sedimentation continued throughout the Cretaceous (Draganits *et al.* 2005). Along the southern Gondwana margin, a Devonian-Permian Gondwana succession overlies the erosional remnants of the late Neoproterozoic-lower Paleozoic orogenic belts (Isbell 1999). The Gondwana section, Devonian sandstone, Carboniferous-Permian glacial diarnictite (Frakes and Crowell 1967, 1969; Frakes *et al.* 1975; Crowell 1978; Craddock *et al.* 2019a), and Permian *Glossopteris-bearing* shale and coal, are deformed, forming a *c.* 250 Ma, thin-skinned, fold belt, known as the Gondwanide orogen, in the Ventana Mountains of Argentina, the Cape Fold Belt of South Africa, the Falkland Islands/Islas Malvinas,

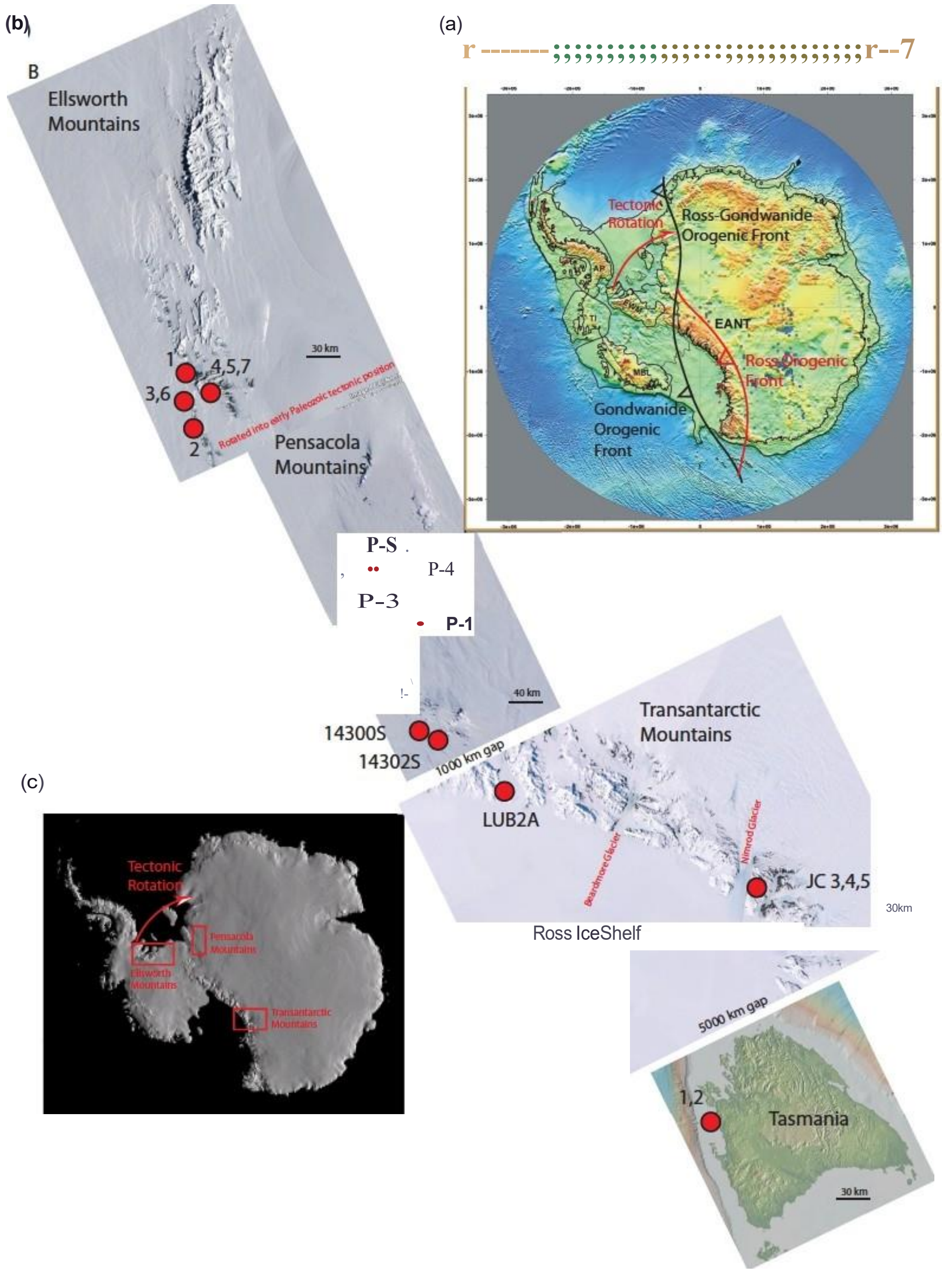

Fig. **4.** Ice-free Antarctica (a) with tectonic provinces (EANT, East Antarctica; EWM, Elsworth Mountains; TI, Thurston Island; MBL, Marie Byrd Land) as a guide for sample sites (**b:** see Table 2) referenced to ice-covered Antarctica (c) and the continuation into Tasmania

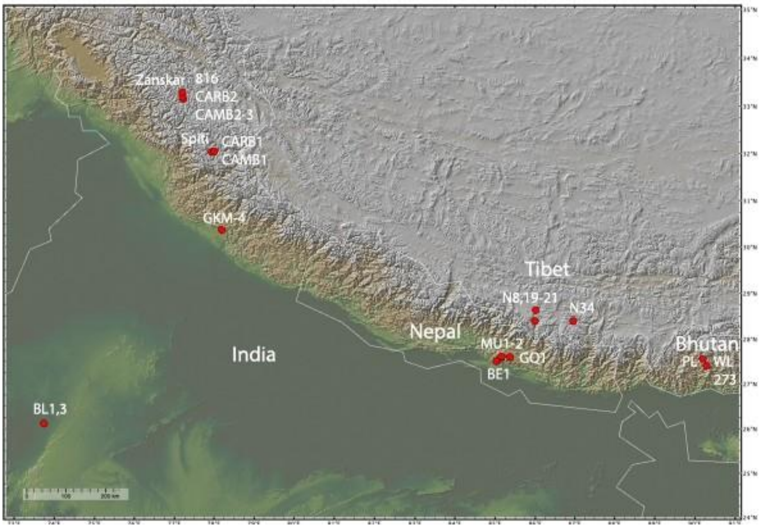

Fig. 5. DEM basemap (GeoApp 3.6.1) of samples sites within the Himalaya and foreland.

and the Ellsworth and Pensacola mountains in Antarctica (du Toit 1937; Craddock 1969, 1982) (Figs 1 & 2). The traceof this fold belt is lost incentral West Antarctica but its outboard presence may explain a change in palaeocurrent directions that are recorded in upper Triassic strata in the undeformed Gondwana section (Beacon Supergroup) in the Transantarctic Mountains (Elliot 2013). Permian-Triassic deformation took place again along the southern Gondwana margin in eastern Australia (Glen 2005). Deformation of the Gondwanide belt was contemporaneous with the Pangaea-forming collision of Gondwana and Laurasia, and the resulting reactivation (inversion) of older structures in Gondwana, namely the Kiri uplift in central Africa (Daly *et al.* 1991), and Laurussia, including the Keweenaw-Kapuskasing uplift in central North America (Malone *et al.* 2016; Craddock *et al.* 2017b).

Methods

Calcite twin analysis

The calcite strain-gauge technique (CSGT) of Groshong (1972) uses the intracrystalline twinning of rock-forming calcite grains to derive a 3Dorientation of stress and strain ellipsoids during twinning. Although the result is a strain tensor, a similarorientation of the stress tensor is calculated in the case of coaxial deformation (Turner 1953, 1962). The CSGT hasbeen used toconstrain 3D stress and strain tensor directions in veins (Craddock and van der Pluijm 1988; Kilsdonk and Wiltschko 1988; Paulsen *et al.* 2014), limestone (Groshong 1975, 1976; Engelder 1979; Spang and Groshong 1981; Wiltschko *et al.* 1985; Craddock and van der Pluijm 1989; Mosar 1989; Ferrill 1991; Craddock *et al.* 1993, 2000, 2007b, 2012), marble (Craddock *et al.* 2017a), amygdaloidal basalt (Craddock and Pearson 1994; Craddock *et al.* 1997, 2004), calcite ocelli in lamprophrye (Craddock *et al.* 2007a) and fault gouge where the calcite has been dated using U-Pb methods (Nuriel *et al.* 2017, 2019; Weinberger *et al.* 2020; Craddock *et al.* 2022). Lacombe *et al.* (2021) reviewed the history and methods of calcite twin analysis.

At temperatures of *c.* 200°C, intracrystalline deformation of calcite results in the formation of e--twins. The formation of calcite e-twins requires a shear stress that exceeds *c.* 10 MPa (Wenk *et al.* 1987; Burkhard 1993; Lacombe and Laurent 1996; Ferrill 1998). Calcite offers three glide systems fore-twinning. From U-stage measurements of the width, frequency and orientation of twins, and thecrystallographicorientation of the host crystals, a strain tensor can be calculated using a least-squares technique (Groshong 1972). To remove 'noise' from the dataset, a refinement of the calculated strain tensor can be achieved by stripping 20% of the twins with the highest deviations (Groshong *et al.* 1984). This procedure has been used where the numberof measured grains was large ($n > 20$). In cases where the data appear to be inhomogeneous, the separation of incompatible twins ('NEV', negative expected values) from compatible twins ('PEV', positive expected values) in the initial dataset allows the separatecalculation of two or more least-squares deviatoric strain tensors. Thus, the CSGT can be used to obtain information on superimposed deformations

(Groshong 1972, 1974) anddifferential stress magnitudes (Rowe and Rutter 1990).

The validityof this stripping procedure was demonstrated in experimental tests where the reliability depends on the overall complexity of deformation and the number of grains with twins (Groshong 1974; Teufel 1980). The stripping procedure was used in cases of high proportions of NEVs and many measured grains. An experimental re-evaluation of the CSGT has revealed that measurements of about 50 grains on one thin section or 25 grains on two mutually perpendicular thin sections yield the best results (Groshong *et al.* 1984; Evans and Groshong 1994; Ferrill *et al.* 2004). The chance of extracting the records of more than twodeformations fromone dataset is limited when dealing with natural rocks (Burkhard 1993). Individual analyses of, for example, veins, matrix and nodules allow the acquisition of sevetal strain tensors without applying statistical data stripping. The complexity of rotational strains in fault zones is limited to the efforts of Gray *et al.* (2005), although the technique is more robust now that calcite can be dated using U-Pb methods (Nuriel *et al.* 2017, 2019). The application of the CSGT requires the following assumptions to be valid: (1) low temperatures (dominance of Type I and Type II twins); (2) random c-axis orientations of calcite; (3) homogenous strain; (4) coaxial deformation; (5) volume constancy; (6) low-porosity materials; and (7) low bulk strain (< 15%). If these conditions are not fully met, calculated strain tensor datasets could be biased, modified or random. Strain tensors were calculated from calcite e-twin datasets using the software package of Evans and Groshong (1994). Fabric interpretations are based on the orientation of the shortening axis (e_1), which usually plots near the contoured maxima of the Turner (1953) axes, and if e_1 is *c.* 20° from the sample bedding, then layer-parallel shortening (LPS) is inferred. Layer-normal shortening (LNS) is the fabric where e_1 isata high angle (>45°) to bedding; vein-normal (VNS) or vein-parallel (VPS) shortening are additional potential fabric interpretations.

Finite strains

Finite strains were measured in quartzite samples using a variation on the centre-to-centre method (auto-correlation function (ACF); see also Owens 1984) as described in Craddock and McKiernan (2007).

Results

Strain results (Tables 1 & 2) are presented fromwest (Ventana Mountains, Argentina) to east (Maria Island, Tasmania) across southern Gondwana (Figs 1-4), then to the Himalayas on the northern margin of Gondwana (Figs I, 2 & 5). In Figures 6-18, field photographs of deformation (Figs 6, 7, 9 & 15) and stereographic plots of strain data (Figs 8, 10-14 & 16-18) for different regions are presented. Summary plots of strain data are provided in Figures 19 (Kurgiakh and Himalayan orogens) and 20 (Buzios, Ross and Gondwanide orogens), with shortening axes projected across Ordovician and Permian platereconstructionsin Figures 21 & 22 (GPLATES: Milller *etal.* 2018).

Sierra de la Ventana Mountains, Argentina

The lower Ventana Mountains expose the contact between Proterozoic crystalline rocks and basal Gondwana section quartzite (Fig. 3) (Buggisch 1987; Cobbold *et al.* 1991; von Gosen *et al.* 1991; Alessandretti *et al.*2013) that have a common structural style across southern Gondwana (Fig. 7). Farther east, in the Ventana foreland, is the Sierra Septionales Range with Proterozoic micritic limestone and younger calcite veins. We sampled the Devonian Ventana Group quartzite in four places and the finite strains preserve a LPS fabric with shortening axes trending easterly; one Proterozoic quartzite sample from the foreland preserves a LPS fabric with shortening directed at 043° (Fig. 8). Fourcalcite veins werecollected, one in the foreland and three in the Ventana Mountains; all preserve a VPS fabric but with a range of orientations.

Caho Frio Terrane, Brazil

The collision between the Sao Francisco Craton (Brazil: Fig. 2a) and the Congo-Angola Craton (Angola and Namibia) spanned the period 540-490Ma, resulting in remarkable ultrahigh-pressure (UHP) tectonites and deformation, including calc-silicates and calcite interlayers (Fig. 9) (Schmitt *et al.* 2004, 2008, 2012; Vieira *et al.* 2022). The peak metamorphic age of 540 Ma places this metamorphism and deformation as partof the final assembly of the interior portions of Gondwana. Metasedimentary rocks of Ediacaran age, preserved as kyanite gneisses interlayered with calc-silicate and amphibolite layers, is refolded in recumbent coaxial north-south fold axes. Calcite twinning strains from two calc-silicate samples record a LPS fabric with the shortening axes parallel to the inferred collisional shortening direction (320°) and no younger Gondwanide strain overprint (Fig. 9). A calcite vein marginal to a Cretaceous mafic dyke (057°, 90°) that formed during the opening of the Atlantic Ocean was also sampled and these twins record shortening parallel to the mafic dyke and the evolving Atlantic margin, with vertical extension.

Table 1. *Strain samples by location*

Location	Finite strain	Limestone	Calcite twinning strains						
			NEV	Vein	NEV	Marble	NEV	Cale-silicate	Totals
Ventana Mountains, Argentina	S			4					9
Rubiera Terrane, Brazil				1				2	3
Cape Belt, South Africa	8	7		12	2				29
Falkland Islands	2								2
Ellsworth Mountains, Antaictica		6	3	2					12
Pensacola Mountains, Antaictica		4		3					9
Nimrod Glacier, Antarctica		2							3
Shackleton Glacier, Antaictica									1
Tasmania		1							1
Himalaya and Foreland, India		9							9
Bhutan		1				2			4
Nepal		1				3			S
Tibet		4				1			S
Totals	15	35	6	23	4	7	0	2	92

Cape Fold Belt, South Africa

Craddock *et al.* *(2001b)* reported calcite twinning strain results for a study of synfolded calcite in the Permian Prince Albert Formation and syndeformational fracture fillings in Dwyka diamictite clasts, both referenced to LPS strains in the nearby foreland to the north. Weinclude theforeland results here, referenced to the finite-strain results for Devonian quartzite in the Cape Fold Belt (Figs IO & 11) (Halbich and Swart 1983; de Wit 1992;Halbich 1992; de Wit *etal.* 1998). All eightquartzite samples preserve LPS fabrics with the shortening axes rotated east from the inferred Gondwanide thrust transport direction (roughly north-south), similar to the results reported in Craddock *et al.* (2007a). The Cambrian carbonates of the Kango window beneath the Cape belt (de Wit *et al.* 1998) are all steeply dipping (roughly east-west, 90°) and the twinning strains of seven limestone samples and two cross-cutting veins were analysed (Table 2). Five limestone samples record north-south horizontal shortening normal to bedding (I.NS). Sample Kango-6 records a LPS fabric with a vertical shortening axis plunge and vertical bedding. Limestone sample Kango-1 strikes SE-NW, 90° with shortening normal to bedding and plunging to the NE. Vein Kango-5 strikes 010°, 90° and preserves a north-south horiwntal shortening strain (VPS) that is also normal to bedding, whereas Kango-6 (vein) strikes 335°, 90° and records a horiwntal shortening strain plunging 20° towards 020° (VNS). The Proterozoic Malmsbury Formation slate in Cape Town is cross-cut by north-south, vertical veins that preserve a north-south horizontal shortening (VPS) strain. None of the samples experienced a twinning strain overprint (low NEVs) despite being exposed under the younger Cape belt. Shortening and extension axis data are plotted for the Ross and Gondwanide orogens for the Cape sample suite (Fig. 12); these data are included in orogen-wide plots (Fig. 20; see the Discussion).

Falkland Islands/ Islas Malvinas

Two samples of the Devonian Port Stanley Formation quartzite (Figs 3 & 7e) were analysed and finite-strain results include two LPS fabrics, both orientated clockwise (*c.* 40°) from the inferred south-directed Gondwanide thrust transport direction (Fig. 14; Table 2).

Ellsworth Mountains, Antarctica

The Ellsworth Mountains are the geographical and tectonic oddity of Antarctica, misaligned from the structural fabric of the Transantarctic Mountains and underlain by Grenvillian crust (Craddock 1969, 1970, 1982;Dalziel andElliot 1982;MillarandPankhurst 1987; Craddock *et al. 2011c)*. The mountains are a north-plunging anticlinorium, exposing *Glossopteris-bearing* Permian strata upsection in the northern Sentinel Range (Craddock *et al.* 1965) and Cambrian strata to the south in the Heritage Range (Webers *et al.* 1992). The Cambrian section

Table 2. *Strain results for the Gondwana margin*

Sample	Rock unit	Calcite rype/age	Orientation	Grains (n=)	£1			£1 (%)	NEV (%)	t,a (bars)	Interpreted fabric	Early Pale.owic inferred thru.1;t Tcmsport direction	Lare Paleoroic inferred thrust Transport direction	Location	C.Omrrent
Siemo de la Ventana, Argentina															
I	Tandi.lla Formation	Vein(Permian	340", 90"	24	351•,9•	082", 5•	203°,80"	--o.2	25	-421.00	VPS		045°	Sierra Septionales Range	Precambrian mkriticLS host
2	SanceGrande Formation	Vein(Permian	101•, 90"	17	193°, 74•	341°, 41°	073•, go	-10.2	17	-400.00	VPS		045°	Abrade la Ventana	
3	SauceGrande FormaLion	Vein/fl,nnian	000", 90"	18	111°, 5•	0860. 60	305°, 82°	-253	27	-357.00	VPS		045°	Sierrade la Ventana	
4	SauceGrande Form.at.ion	Vein(Permian	337°, 90"	17	338", 3•	070", 17°	236,o, 72•	--o.3	II	-322.00	VPS		045°	Sierrade la Ventana	
V-1	Quartzite	Ptote.rowic	Horimntal	ACT'	043•, r	129°, 5•	26Jo, 860	1.1:1:0.88			LPS		045°	SierraSept. Range	
V-3	Quartzite	Devonian	321•,4rw	ACT'	u,r, 44•	133°, 38"	037°, go	1.13:1:0.87			LPS		045°	Peralta	
V-4	Quartzite	Devonian	334°,62°W	ACT'	U,3°, 64°	141°, 12°	053°, 4•	1.21:1:0.78			LPS		045°	Ce1TO Bahia Blanca	
V-6	Quartzite	Devonian	328°, 25•w	ACT'	07go, 4°	1830, 360	337°, 24•	I.I I:1:0.92			LPS		045°	Abrade la Ventana	
V-9	Quartzite	Devonian	338", 24•w	ACT' n=76	os1•, r	354•, r	227°, 84•	1.23:1:0.86			LPS		045°	Pan de Azuca	
Brazil															
B-1	Proterozoic	Cale-silicate/ Cambrian	060", 65°S	33	31go, 9°	22S\ 86°	062°, 3•	-3.4	15	-342.00	LPS	320"		Caho Frio	
B-2	Cretaceous dyke	Dyke-margin vein	05r, 90"	37	235•, r	352°, 4	13go, 82°	-5.8	4	-374.00	VPS	320"		Caho Frio	
B-3	Proterowic	Cale-silicate/ Cambrian	Horimntal	29 n=99	322°, 5•	0710, 350	231°, 6°	–32	6	-397.00	LPS	320"		Buzio	
Cape Fold Belt, South Africa															
I	Prioce Albert funnat.ion	IS/llmnian	Horizontal	34	0010, 50	osr, 5•	181•, 87°	-45	7	-341.00	LPS		000"	Karro fut-eland	Craddock ,i al (2007a)
Iv	Prioce Albert Formation	Vein(Permian	000", 90"	22	351°, 12°	063°, 3°	210", 86°	-9.2	18	-389.00	LPS/VNS		000"	Karro fut-eland	Craddock ,t al (2007b)
2-PBV	Prioce Albert ronnalion	Vein/fl,nnian	090", 35°S	48	211°,22°	osr. ,r	350", r	--o.15	0	-712.00	LPS		000"	Foldstudy; liroo	Craddock et al (2007a)
2-NEV	Prioce Albert rormation	Vein(Permian	090", 35• S	19	067°, 65°	168°, 5•	212°, 21•	-7.99	100	-718.00	LNS		000"	Foldstudy; liroo	Craddock e, al (2007b)
3-PBV	Prioce Albert furmat.ion	Vein/Permian	Horimntal	43	175°, 14°	u,1•, 47°	045°, 31•	-3.65	0	-721.00	LPS		000"	Foldstudy; hinge	Craddock e, al (2007a)
3-NEV	Prioce Albert Mlrnlation	Vein/fl,nnian	Horizontal	23	251•, 71•	055•, 11·	322°, 12•	-3.76	100	-725.00	LNS		000"	Foldstudy; hinge	Craddock e, al (2007b)
4	Prince Albert furmat.ion	Vein/Permian	090", 35• N	65	357°, 28°	0910. 120	177°, 64°	--o.4	2	-323.00	LPS		000"	Foldstudy; liroo	Craddock et al (2007a)
5	Prince Albert rormation	Vein(Permian	090", 35°N	24	028°, 31°	104•, r	201•, 76°	-5.8	0	-371.00	LPS		000"	Foldstudy; liroo	Craddock et al (2007b)
6	Dwyka	IS Clas./ Cambrian?	N/A	25	000", 15•	11go, 55•	088°, 35•	-4.6	0	-342.00	CNS		000"	Cleavage study	Craddock ,r al (2007a)
7	Dwyka	Vein(Permian	090", 90"	24	192°, 2°	300", 62°	121•, 19°	-5.1	0	-562.00	CNS		000"	Cleavage study	Craddock ,r al (2007b)
8	Dwyka	Fibroos Vein/ Perm	Horirontal	25	182°, 4°	011°. 81°	282°, ,.	-4.8	0	-482.00	CNS		000"	Cleavage study	Craddock ,i al (2007a)
C.composite (6,7,8)	Dwyka	Composite/Penn	Corooined	74	181°, i-	350", 88°	091°. 3°	-5		-465.00	CNS		000"	Cleavage study	Craddock ,1 al (2007b)
K.ngo 3-3	K.ngo Inlier	Vein/Cambrian	090", 90"	21	oor,3•	302°, 5•	182°, 86°	-2.3	0	-411,.00	LNS	000"		Kango Inlier	deWit ral. (1998)

(Cntinued)

Table 2. *Continued.*

Sample	Rock unit	Calcite type/age	Orientation	Grains (n=)	e,	e,		s, (%)	NEV (%)	t,q (bars)	Interpreted fabric	Early Paleomic infern,d thrust Ttansport direction	Late Paleomic inferred thrust Transport direction	Lcx:ation	C.Omrrent
	KangoInlier	LS/Cambrian	300", 90"	35	044'\ '.31°	271'\ 5°	178°, Z7"	-M	6	-384.00	INS	000"		Kango Inlier	de Wit *etal.* (1998)
2	KangoInlier	LS/Cambrian	090", 90"	34	001°. 21°	156•, Ill°	252", 38°	--6	5	-397.00	INS	000"		Kango Inlier	de Wit *ti al.* (1998)
3	Kango Inlier	LS/Cambrian	090", 90"	64	344•, 37"	167", 51•	248", r'	-3.6	3	-402.00	INS	000"		Kango Inlier	deWit *etal.* (1998)
5	Kango Inlier	Vein/Caniirian?	010", 90"	23	001•, 17"	m°. 21°	171°. 81°	-7	9	-412.00	INS	000"		Kango Inlier	deWit *et al.* (1998)
6	Kango Inlier	LS/Cambrian	090", 90"	19	167", 86·	283•, 2"	013•, 3•	--6.2	5	-384.00	VPS	000"		Kango Inlier	de Wit *eta/.* (1998)
6v	KangoInlier	Vein/Caniirian?	335•, 90"	15	020", 20"	308°, 12"	186•, 62"	-2.7	0	-425.00	IPS	000"		Kango Inlier	de Wit *et al.* (1998)
8	Kango Inlier	LS/Cambrian	090",90"	28	354•, 21•	122•, 44•	213•, 34•	-4.6	18	-411.00	VNS	000"		Kango Inlier	deWit *ttal.* (1998)
Kango4-5	Kango Inlier	Vein/Caniirian?	(177",90"	25	170", 14•	208°, 12"	351°, 84°	-IO.I	25	-380.00	INS	000"		Kango Inlier	de Wit *eral.* (1998)
MQ5	MQ5	Vein/Slate	000",90"	43	357", 3•	UIJ", 3•	1000. 860	-14.1		-372.00	VPS	000"		Quany,Cape Town	Proterozoic host
CFBI•1	TableMountain Group	Devonian	Horimntal	ACF	032", 4•	308°, go	131•, 31•	1.12:1.0:.88			LI'S		000"	North Helshoo!ge Pass	de Wit *etal.* (1998)
CFBI-5	TableMountain Group	Devonian	Horimntal	ACF	0210. 30	288°, 6·	179", 82"	1.22:1.0:.89			LI'S		000"	NuyThru.1;t	deWit *etal.* (1998)
CFBI-7	TableMountain Group	Devonian	090", 90"	ACF	248", 77"	348°, 12"	(174•, 9"	1.17:1.0:.92			LI'S		000"	Koogman's Kloof	deWit *er al.* (1998)
CFB3-2a	TableMountain Group	Devonian	088°, 78°S	ACF	251•, 68°	341'\ 23°	094•, go	1.21:1.0:.90			IPS		000"	Seveowee.kspoon	deWit *eral.* (1998)
CFB3-2b	TableMountain Group	Devonian	094•, 47"S	ACF	227", 43•	(176•, 31•	302", 23•	1.17:1.0:.86			IPS		000"	SevenweeksJX)Ort	deWit *eta!.* (1998)
CFB3-3	J\:.ninsula Formation	Devonian	087",45•S	ACF	241•, 33•	088°, 16·	344•, 5•	1.22:1.0:.84			IPS		000"	Calittdorp	de Wit *eral.* (1998)
CFB4-5	VartwellR>rrmtion	Devonian	091•, 72"S	ACF	252", 68°	131°. 14°	012", 22"	1.16:1.0:.93			IPS		000"	Boplaas	deWit *etal.* (1998)
CFB4.JO	ninsula Fonnat.K>n	Devonian	087",82°S	ACF	244°. 71°	301•, 17"	(179", 21•	1.18:1.0:.86			IPS		000"	Swart:zberg Fliss	de Wit *etal.* (1998)
				•=733											
Falkland Islands															
I	R:irt Stanley Fonnation	Devonian *Qtw*	090",90"	ACF	092", 42"	233•, 41•	188", 6·	1.24:1:.93			IPS		000"	Stanley	
2	R:irt Stanley Formation	Devonian *Qtw*	Horizontal	ACF	290", go	186•, 30"	035•, 58°	1.14:1:.83			IPS		000"	WestIsland	
Ellsworth Mountains, Antardia,															
I	Minaret Limestone	LS/Cambrian	090", 32"S	22	211•, Ill°	3010. 30	036•, 88"	-11.2	20	-357.00	IPS	090"		Soholt Peaks	Craddock ,r *al* (2017c)
2v	Minaret Limestone	Vein/ Canilrian	021•,56•E	24	018°, 8°	118°, 18°	308°, 34•	-II.I	12	-555.00	VPS	090"		Mowit Fordell	Craddock ,r *al* (2017b)
3	Minaret Limestone	LS/Cambrian	235•,63•5	76	167", 67"	321°. 5°	0240. 210	-12.6	25	-400.00	IPS	090"		Minaret hale	Craddock *et al* (2017a)
3-NEV	Minaret Limestone	LS/Cambrian	285•, 63•S	19	052", 36•	318°, 6·	219", 53•	-3.1	100	-400.00	LNS	090"			Craddock *et al* (2017c)

4	**Minaret Limestone**	LS/Cambrian	290", 40"S	71	**251°, 31°**	168", 4°	0!,7", 14°	125	28	-555.00	LI'S	090"		Mount Fordell	Craddock *eral* (2017b)
4-NEV	**Minaret Limestone**	LS/ Cambrian	290", 40"S	20	095°, 27°	274°, 5°	183°, 31°	-6.9	100	-555.00	LNS	090"			Craddock *,1 al* (2017a)
5	**Minaret Limestone**	LS/Cambrian	290", 40"S	35	**214"\ 26°**	312°, 15•	117°, 52°	-3.3	41	**-588.00**	LI'S	090"		Mount Fordell	Craddock *,r al* (2017c)
5-NEV	**Minaret Limestone**	LS/Cambrian	290", 40"S	14	141°, 32°	237°, 12°	357°, 84°	-8.3	JOO	-588.00	LI'S	090"			Craddock *,r al* (2017b)
6	**Minaret Limestone**	LS/Cambrian	2ss·. 41°s	27	193°, 22°	274°, 8°	012°, 87°	-13.4	18	-588.00	LI'S	090"		**Minaret Peak**	Craddock *et al* (2017a)
6v	**Minaret Limestone**	Vein/Cambrian	340", 90"	38	018°, 11°	277°, 12°	169°, 41°	-4.3	40	-555.00	VNS	090"		**Minaret Peak**	Craddock *,r al* (2017c)
6v-NEV	**Minaret Limestone**	Vein/Cambrian	340", 90"	15	n1°. 81°	**243°, 3°**	334°, 8°	-4.1	JOO	-555.00	VPS	**090"**			Craddock *,r al* (2017b)
7	**Minarer: Limestone**	LS/Cambrian	298°, 44°S	37	220·. 38°	**113'\ 21°**	312°, 52°	-6.3	7	-458.00	LI'S	090"		Mount Fordell	Craddock *,r al* (2017a)
8	**Minaret Limestone**	Striared thrust gouge	300°,20°W	37	247°, 21°	147°, 5°	317°, 84°	-6.4	4	-384.00	LI'S	**090"**			Craddock *et al* (2019a)
				n=435											
l'l,nsacola Mountains, Transantardic Mountains, Antarctica															
P-1(PEV)	**NelsonLimestone**	Vein/Cambrian	041°, 90"	30	**0450, 40**	138°, 12°	227°, 81°	-4.8	50	-302.00	VPS	110"		R74l5	British **Antarctic** Survey samples
P-1 (NEV)	**Nelson Limestone**	Vein/Cambrian	041°, 90"	15	223°, 12°	127°, 7°	318°,88°	-5.2	100	-343.00	VPS	110"		R74l5	
p.3	**Nelson limestone**	Vein/Cambrian	335°, **90"**	25	257°, 87°	178°, 6°	**091°. 3°**	-15	16	-350.00	VPS	110"		R7435d	
P-4 (NEV)	**Nelson lime.gone.**	**Conglomerate**	031°, 80"W	48	284°, 63°	026°, 18°	**153°. 41°**	-6.3	38	-337.00	LI'S	110"		R7433-7a	
P-4 (PEV)	**Nelson limestone**	**Conglomerate**	031°, 80"W	18	172°, 51°	073•, 9°	337°, 43°	*-52*	100	-331.00	VPS	110"		R7433-7a	
p.5	**Nelson Limestone**	Vein/Cambrian	082°, 79°S	33	**0SS0. 140**	233°, 31°	338°, 17°	-8.2	16	-353.00	VPS	110"		R7435B	
143005	**Nelson limestone**	LS/Cambrian	087°, 57°S	*28*	011°, 42°	118°, 18°	226°, 42°	-2.9	7	-217.00	LNS	110"			
14302$	**Nelson limestone**	LS/Cambrian	079°, 53°S	25	143°, 39°	332°,51°	**236°, 4°**	-15	15	-202.00	LI'S	110"			
				n=222											
Nimrod Glacier, Transantardic Mountains, Antarctica															
JC[illegible]	ByrdGroup	Vein/Cambrian	038°, 90"	22	135°, 22°	214°, 4°	313°, 88°	-9.9	0	-350.00	VNS	070"			
JC4a	ByrdGroup	Vein/Cambrian	031°, 70"SE	26	018°, 12°	112°, 58°	**274°, 23°**	-2	34	-354.00	VNS	070"			
JC4b	ByrdGroup	LS/ Cambrian	**Notwi**												**MICrite**
JCS	ByrdGroup	LS/ Cambrian	**Horizontal**	30	177°, 3°	357°, 87°	088°, 2°	-2.1	3	**-366.00**	LI'S	070"			
				n=78											
ShackJeton Glader, Tramantardic Motmta Antarc ica															
LUB2A	Liv Group	MBL/Cambrian	022°, 66°SE	25	268·. 8°	1730, -u,0	on•.61°	-4.6	15	-243.00	LNS	090"			
				n=25											
Tasmania															
I	**Panneener Group**	LS/1'1,nnian	**Horimntal**	33	344°, 6°	078°, 7°	244•, 88°	-3.4	7	-358.00	LI'S		270"		
2	**Parrne.eoer Group**	Vein/1'1,nnian	092°, **90"**	42	352°, 4°	083°, 5°	191°, 87°	-7.1	*5*	-397.00	VNS		270"		
				n=15											
India															
GKM-4		fuliated LS/ Creraoeous('))	228°,38° NW	18	045°, 32°	313°, 4°	218°, 59°	-2.7	4	-211.00	LI'S			Gopi Chand Ka Mahal	
BL!	**Bilara Limestone**	LS/Fdiacaran	007°, ss·sE	58	219°, 32°	324°, 23°	83°, 49°	-1.6	23	-231.00	LNS	220° (Kurgiakh Orogen)		**MarwarBasin**	
BL3	**Bilara Limestone**	LS/Fdiacaran	048°,9°SE	28	224°, 12°	346•, 69°	128°, 16°	-2.1	3	-228.00	LI'S	220° (Kurgiakh Orogen)		**Marwar Basin**	
CARil!	Lipiak funnation	LS/Carboniferous	335°, 23°E	43	056•, 30°	298°, 39°	172°, 36°	-9.14	9	-274.00	LI'S			Parahio Valley	**P.mlsen *el al*** (2007b)
CAMBI	**Parahio funnatK>n**	LS/Cambrian	354°, 37°E	42	()1.,6•, 25•	158°, 55°	**285'\ 23°**	-858	19	-256.00	LI'S	220° (Kurgiakh Orogen)		Parahio Valley	**Paulsen *el al*** (2007a)
81601-1	LilangG10up	LS/1'1,nnian-Tri.as.sic	272°, IS°N	40	056°, 15°	**323°. 14°**	187°, 71°	-4.3		-263.00	LI'S			Zanskar VaUey-Tsarap River	

(Continued)

Table 2. *Continued.*

Sample	Rock unit	Calcite type/age	Orientation	Grains (n=)	e,	e,		s, (%)	NEV (%)	t,q (bars)	Interpreted fabric	Early Paleomic infern,d thrust Ttansport direction	Late Paleomic inferred thrust Transport direction	Lcx:ation	C.Omrrent
CARB2	Lipiak Formation	LS/Carboniferous	354•, 37"E	43	090", 5•	210", 80"	359", 8"	-8.6	IO	-190.00	lPS			Zanskar Valley	P.mlsen el al (2007b)
CAMB2	Kurgiakh Formation	LS/Cambrian	030",43•E	40	080", 6·	180", 58"	346•, 32"	-4.88	7	-236.00	LP$	220" (Kurgiakh Orogen)		Zanskar VaUey	Paulsen et al (2007a)
CAMB3	Kurgiakh Fonnatkm	LS/Cambrian	047", 39"S	40	206°. 4°	115, 18"	309", 71•	-851	17	-269.00	LP$	220" (Kurgiakh Orogen)		Zanskar VaUey	P.lulsen n al (2007b)
				•=352											
Nepal															
GQI (ffiV)	O>andragiri Limestone	LS/Silurian	I02", 86•N	22	126°. 4°	008", 82"	217", 7"	-I.I	II	-155.00	LP$			Godovari Valley	
GQI (NEV)	O>andragiri Limestone	LS/Silurian	I02", 86•N	18	214•, J6•	118", 22"	337", 62"	-1.2	100	-145.00	LNS			Godovari Valley	
BEi	Bhaisni Marble Neoproterozoic?	MBL/ 294•,69"N	22	012•. 29"	194•, 61•	103°.)°	-1.3		-193.00	LPS	220·	(Kurgiakh Orogen)		Bhai.sni	
MUI	Marku Limestone Neoproterozoic?	MBL/ 314•, 47"N	25	1io•, 57"	239", 23•	339", 24•	-3.1	22	-242.00	LPS	220·	(Kurgiakh Orogen)		Godovari Valley	
MU2	Mark:u Limestone Neoproterozoic?	MBL/ 125•, 38"N	1.6	344• 82"	18)•, 8"	091•, 2"	-1.9		-180.00	LNS	220·	(Kurgiakh Orogen)		Godovari Valley	
				•= 113											
Tib<t															
N34		LS/Pennian	IOO", 34•N	1.6	005•, 30"	104'\ 14°	216·, 56•	-1.9	17	-165.00	LP$			Nyalam	
N21	Chiatsun Groop	LS/Ordovician	253•, 30"N	23	213•, 43•	338", 32"	089", 31•	-I.I	17	-189.00	LNS			Nyalam	
N2()	Chiatsun Groop	LS/Ordovician	253•, 30"N	30	192", 17"	076•, 43•	298", 43•	-1.3	21	-167.00	LNS			Nyalam	
Nl9	Chiatsun Groop	LS/Ordovician	109", 49"N	1.6	036•, 18"	238", 72"	128", 6·	-3.2	16	-198.00	LP$			Nyalam	
NS	NorthCol Formation	MBL/Cani>rian	238",57"N	35	158", 34•	056•, 17"	304•, 51•	-I.I	5	-174.00	LNS	220" (Kurgiakh Orogen)		Nyalam	
				•= 140											
Bhutan															
WL9_9_02 (ffiV)	Wochi La Format.ion	LS/Ordovician-Siturian	252", 6•N	42	058", 2"	152", 49"	31.6•, 41•	-2.2	0	-202.00	LP$			Black Mountain	
WL9_9_02 (NEV)	Wochi La Fonnation	LS/Ordovician-Sitwian	252",6•N	30	324•, 32"	156•, 58"	056•, 4•	-1.3	100	-191.00	LP$			Black Mountain	
Pl.A	PeleLa Group	MBL/ Ordoviciao-Silurian?	025•, 9"S	7I	)860. 250	()66•, 47"	2930. 330	-1.7	0	-2I0.00	LP$			Black Mountain	
?:13.74	Quamite Fonnat.K>n	MBL/upper Cambrian?	Horizontal	41	082", 19"	350", 7"	242", 69"	-I.I	II	-181.00	LP$	220" (Kurgiakh Orogen)		Black Mountain	
				•= 140											
				Total: 2488											

Key: ACF, auto-oorrelation function (finite strain); LPS, layer-parallel shonening; LNS, layer-normal shonening; VPS, vein-parallel shonening; VNS, vein-normal shonening; CNS, clast-nonnal shonening (Dwyka clasts).

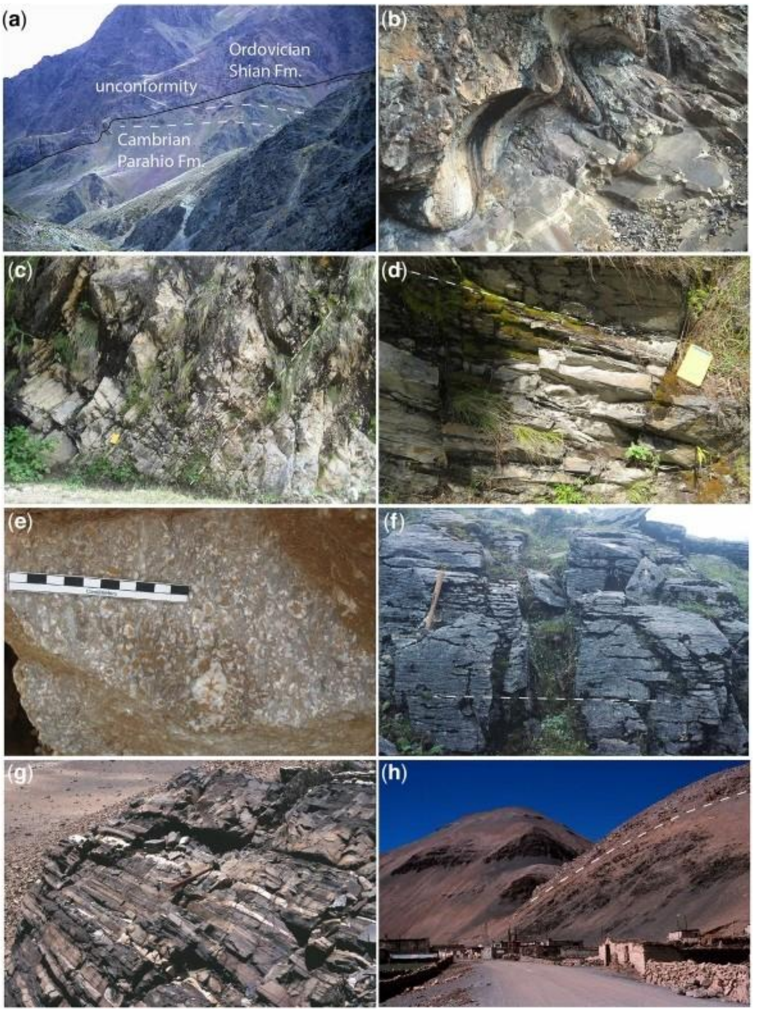

Fig. 6. Field photographs showing Himalayan sections. **(a)** Angular unconformity separating the Cambrian Parahio Formation and the overlying Oniovician Shian (previously referred to as the Thango Formation) in Parahio Valley, India. **(b)** Oose-up showing scours in the Parahio Formation (below) along the unconformity in (a). (c) Dipping Neoproterozoic Bhaisni Marble at Bhaisni [sic], Nepal. (d) Dipping Marlen Limestone in Godovari Valley, Nepal. (e) Oniovician-Silurian(?) Chandragiri Limestone in Godovari Valley, Nepal. **(f)** Oniovician-Silurian(?) carbonates at Black Mountain, Bhutan. (g) Dipping Cambrian carbonate (white) intetbedded with siliciclastic rocks near Nyalam, Tibet. **(h)** Dipping upper Paleozoic (Mississippian) stratigraphic succession near Nyalam, Tibet

is estimated to constitute half of the 13 000 m-thick stratigraphic succession, ischaracterized by a diverse middleCambrianfauna (Craddock andWebers 1964; Webers *et al.* 1992), and includes the Upper Cambrian Minaret Formation Limestone (*c.* 500 m) and calcite veins. The classic Gondwana section unconformably overlies the Cambrian section (Duebendorfer and Rees 1998). Structural studies reveal east-vergent folding along west-dipping thrusts with a well-developed axial-planar cleavage and local, top-to-the-east kinematic indicators (Fig. 7c) (Craddock *et al.* 1992; Sporli and Craddock 1992; Curtis 1998; Curtis *et al.* 1999; Craddock *et al.* 2017b). Our calcite strain results were presented in Craddock *et al.* (2017a, *2019b,* fig. 4) and include six Minaret Limestone samples with LPS fabrics; three of the limestones have twinning strain overprints (two LNS fabrics and one LPS fabric). Two calciteveinsrecordrange-parallel horizontal shortening (VPS fabric); one vein has a strain overprint that records vertical shortening. One sample was striated fault gouge calcite sampled along a thrust fault that

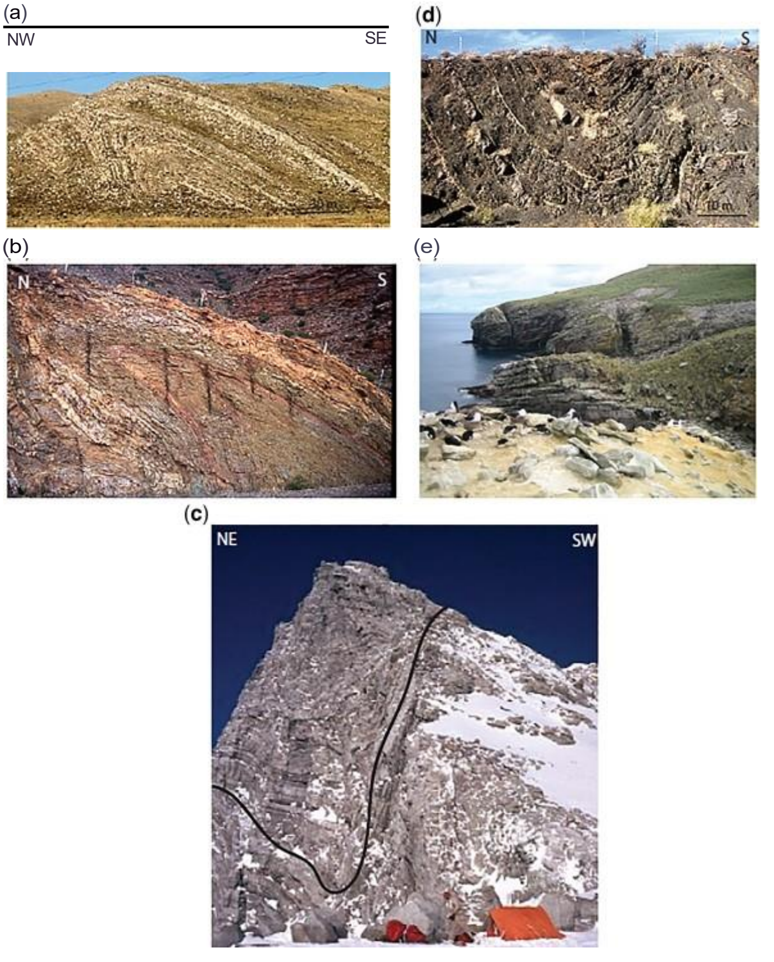

Fig. 7. Field photographs of Gondwanide deformation. (a)-{c) Asymmetrical folds in Devonian quartzites in the Ventana Cape (fence posts are for scale) and Ellsworth Mountains, folds in the northern Cape belt (d: see Craddock *et al* 2007) and dipping Devonian quartzites, Falkland Islands (e: the penguins are for scale).

offsets both the Minaret Limestone and a breccia body, and is presumed to be related to Gondwanide deformation. Summary plots of the Ross and Gondwanide deformation for the Ellsworth Mountains are provided (Fig. 13).

Pensacola Range, Transantarctic Mountains, Antarctica

The Pensacola Mountains are the southern extension of the Ellsworth Mountains Block (Fig. 4) in the Transantarctic Mountains, and include lower Paleozoic strata that are gently folded (east vergence) and weakly cleaved (Millar and Storey 1995; Stump 1995;Storey *etal.*1996;Curtis*etal.* 2004).Six Cambrian Nelson Limestone samples were analysed: two are limestone, one is a conglomerate (calcite cement matrix) and three are veins of different orientations (Fig. 14). One limestone preserves a SE-plunging LPS shortening strain, whereas theother sample preserves a north-plunging LNS shortening strain. The conglomerate preserves a subvertical shortening strain (51° plunge) with a twinning strain overprint that plunges 63° and trends 090° away from the primary (PEV)shortening strain.Vein P1 records a subhorizontal shortening strain orientated to the NE with a twinningstrainoverprint(PI-NEV)orientated to the SW, with the extension and intermediate strain axes reversed. Vein P5 is orientated approximately east-west with a 79°S dip and records layer-parallel, east-west shortening strain with no overprint. Vein P3 (335°, 90°) records a vertical shortening strain

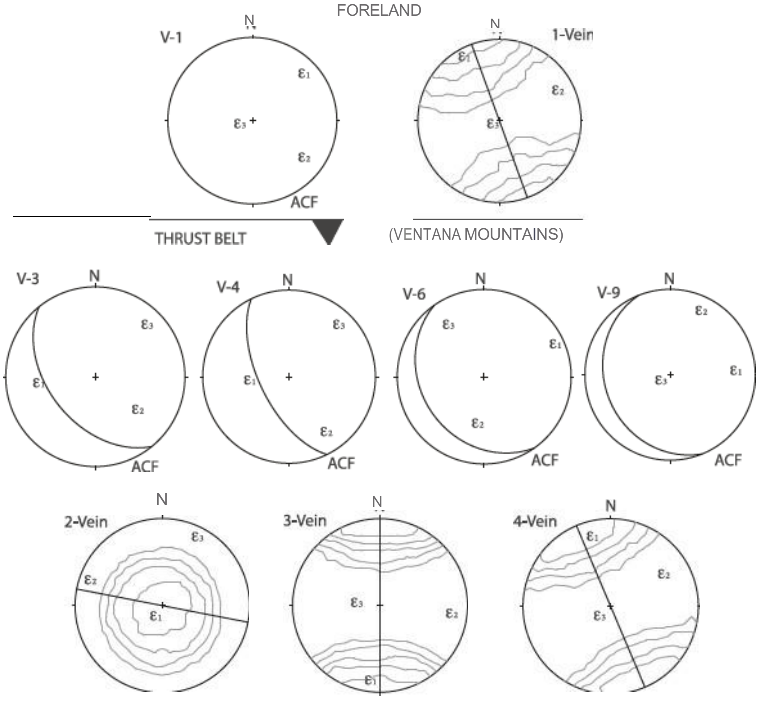

Fig. 8. Strain data for the Ventana Mountains and foreland, Argentina. Finite strains (ACF method) are from quartzites, and calcite twinning strains are from veins (see Table 2). Key: ε_1, shortening axis; ε_2, intennediate axis; ε_3, extension axis with compression axescontoured for the twinning data

with no overprint. The limestone and conglomerate LPS fabrics areconsistent, with Ross shortening at a high angle to the structural grain with a vertical overprint. The younger vein fabrics record vein-parallel shortening (VPS) but in a myriad of orientations.

Shackleton Glacier, TransantarcticMountains, Antarctica

The Cambrian Liv Group in the Queen Maud Mountain sector of the Transantarctic Mountains includes subgreenschist- to amphibolite-facies metasedimentary and metavolcanic rocks that exhibit varying degrees of folding, axial-planar cleavage development and local shear-zone development. The Liv Group and associated intrusive rocks are separated, unconformably, from the flat-lying Devonian-Permian Beacon Supergroup above (Fig. 15). Our sample (LUB2A) comes from the Cambrian Taylor Formation of the Liv Group (Stump 1982, 1986, 1995; Paulsen *et al.* 2018) at Lubbock Ridge along the Shackleton Glacier, where east-dipping metamorphosed limestone (marble) is interbedded within siliciclastic metasedimentary rocks (Fig. 4). Detrital, volcanic and intrusive U-Pb zircon ages constrain folding to have taken place between *c.* 522 and 496 Ma at this locality (Paulsen *et al.* 2021). Calcite twins within sample LUB2A preserve horizontal east-west LNS at a high angle to the north-south fold axes, and cleavage of the Ross orogen with a single compression axis maxima indicates a simple twinning record (Fig. 16).

Nimrod Glacier, Transantarctic Mountains, Antarctica

The Cambrian Byrd Group in the Transantarctic Mountains includes the Shackleton Limestone, which is broadly equivalent to the Cambrian Nelson Limestone and Liv Group found in the Pensacola Range (Stump 1992). The Byrd Group was deformed in the Cambrian-Ordovician during the Ross Orogeny (Myrow *et al.* 2002; Goodge *et al.* 2004a, *b;* Paulsen *et al.* 2007b, 2008). It rests unconformably below the younger, flat-lying Devonian-Permian Beacon Supergroup (Fig. 15) (Isbell 1999). Our samples come from the Nimrod Glacier area (Fig. 4) and include one limestone and two cross-cutting veins. Sample JC-5 is from a flat-lying limestone and preserves a twinning shortening strain parallel (north-south) to the mountain range. Vein JC-3 (038°, 90°) records a horizontal shortening strain normal to the vein (VNS fabric) and at an

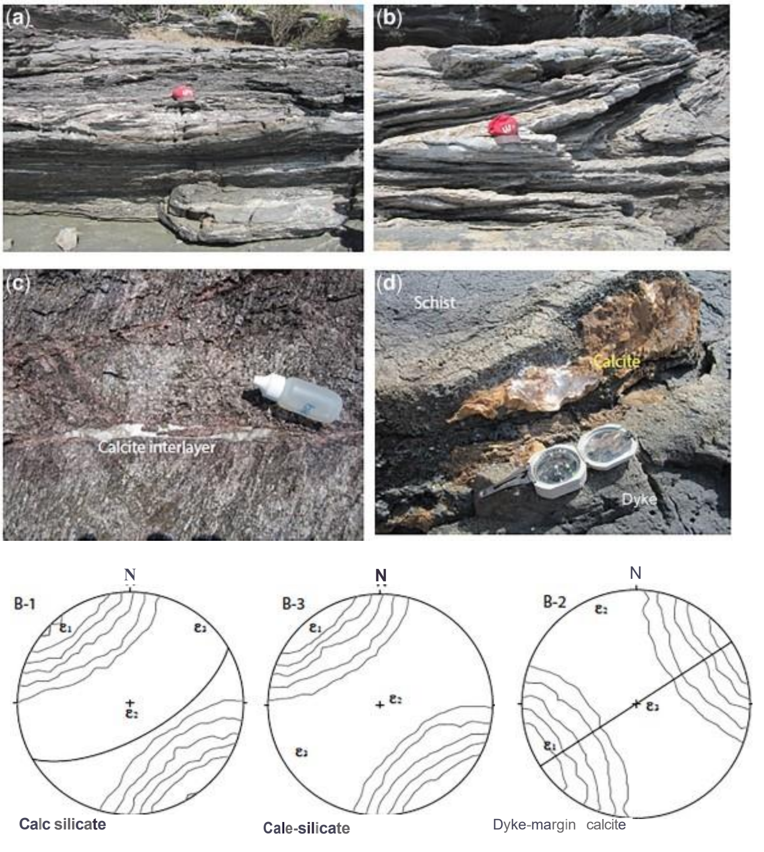

Fig. 9. (a}-(c) Field photographs from the Cabo Frio Terrane, Buzios orogen, Brazil. Cale-silicate layers are boudinaged and subsequently folded in recumbent structures with north-south axes. (d) Calcite vein marginal to a NE-SW Cretaceous dyke. Lower-hemisphere projections of calcite strain data with principal strain axes and contoured compression axes (see Table 2).

acute angle to the mountain range. Vein JC-4 (031°, 71°SE) records a horirontal shortening strain 45° to the vein (VNS) and normal to the shortening strain in vein JC-3 (Fig. 16).

Tasmania

One limestone sample was collected from the Permian Parmeener Formation on Maria Island and includes a sampled calcite vein (Fig. 4). The limestone and vein (092°,90°) both record a subhorizontal shortening strain in the inferred east-westdirection of Gondwanide orogenic shortening (Fig. 16).

The upper Neoproterozoic-Cambrian Hairnanta Group in the Zanskar and Spiti sectors of the NW Himalaya of India (Fig. 5) includes low-grade (diagenetic to low--epizone facies) interbedded sandstone and limestone (Dezes 1999; Wiesmayr and Grasemann 2002; Myrow *et al. 2006a, b)*. The Haimanta Group and associated 552-479 Ma intrusive rocks are separated, unconformably, from an Ordovician conglomerate by an angular unconformity attributed to uplift and exhumation associated with the Kurgiakh Orogeny (Fig. 6a, b) (Hayden 1904; Garzanti *et al.* 1986; Dezes 1999; Miller *et aL* 2001; Wiesmayr and Grasemann 2002; Myrow *et al. 2006a, b,* 2016). The conglomerate, in turn, is succeeded by an Ordovician-Cretaceous sedimentary succession that includes Early Permian Panjal Traps and unconforrnities associated with rifting and theformation of the Neo-Tethys Ocean (Draganits *et al.* 2005). The entire succession has been deformed by NW-SE-trending, SW-vergent folds, associated cleavage and thrusts formed during the Cenozoic evolution of the Eohirnalayan Tethyan fold-thrust belt (Wiesmayr and Grasemann 2002). Paulsen *et aL* (2007a) reported calcite twinning strain results for a study

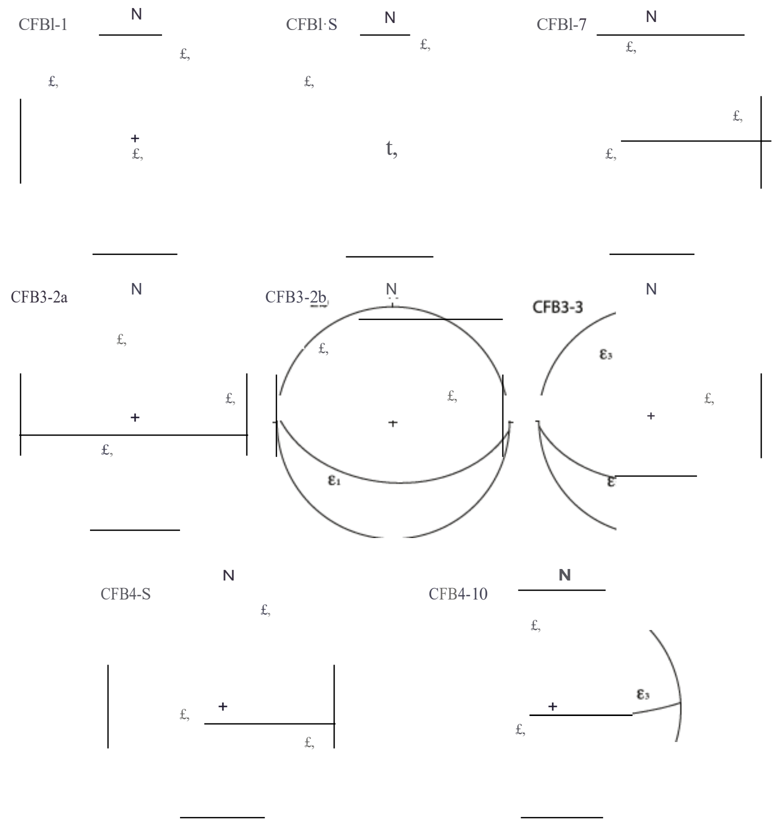

Fig. 10. Lower-hemisphereprojections of finite-strain (ACF: see Table 2) data for the Cape Fold Belt Great circles are bedding; *ei,* shortening axis; e_2,interrnediate axis; e_3, extension axis.

of Cambrian (n = 3) and Carboniferous (n = 2) limestone samples collected across the Cambrian-Ordovician Kurgiakh unconformity in both the Spiti and Zanskar areas in order to compare strain patterns associated with early Paleozoic and Cenozoic orogenesis. Cambrian samples yield NE-SW to east-west LPS fabrics that are roughly paralJel to LPS fabrics in Carboniferous rocks (Fig. 17). These shortening strains are similar in orientation to four new calcite twin strain analyses reported here that include a Permian-Triassic Lilang Group limestone from Zanskar (sample 81601-1), a sheared recrystallized limestone of possible Cretaceous age from Gopi Chand Ka Mahal in the lesser Himalaya (sample GKM-4) and two Ediacaran limestone samples collected from soft-sedimentary folds in the Bilara Formation (Chakraborty *et al.* 2019) in the Marwar Basin of the Indian Shield (samples BL-I and BL-3) (Fig. 5). The Himalayan orogenic belt samples and Indian Shield sample BL-3 yielded NE-SW LPS fabrics, whereas shield sample BL-1 yielded a NE-SW LNS strain plunging 32° towards 224° (Fig. 17). Three of these samples (81601, GKM-4 and BL-1) show single compression axis maxima, indicating a simple twinning record; however, GKM-4 possesses a limited rangeof c-axis orientations and should therefore be viewed with some caution. Sample BL-3 shows bimodal compression axis maxima, indicating a complex twinning history.

Nepal

Rocks of the Kathmandu Klippe in the Nepalese Himalaya (Fig. 5) include upper Neoproterozoic-middle Paleozoic strata that were thrust southwards over Proterozoic siliciclastic rocks of the Lesser Himalaya and subsequently folded into the NW-SE-trending Kathmandu synform (Gehrels *et al.* 2003, 2006; Cawood *et al.* 2007). The stratigraphic succession of the thrust sheet is divided into two successions that include: (1) schist, marble and quartzite of theBhimpihedi Group; and (2) unmetamorphosed sandstone, shale and limestone of the Phulchauk:i Group (Gehrels *et al.* 2006; Cawood *et al.* 2007). Age constraints provided by Th/Pb monazite inclusions in metamorphic garnet, and U-Pb zircon

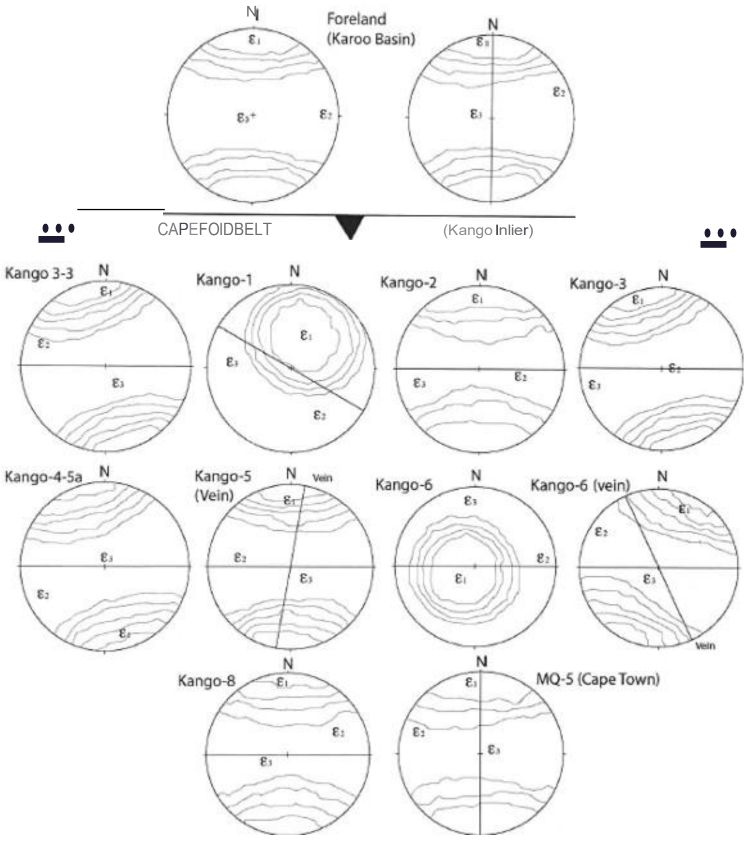

Fig. **11.** Lower-hemisphere projections of calcite strain data for theCape Fold Belt foreland (upper two stereonets; see Craddock *et al.* 2007*b*), and Cambrian limestones and veins of the Kango Inlier. Key: Great circles are bedding or vein orientations; ε_1, shortening axis; ε_2,intennediate axis; ε_3, extension axis.

ages for intrusions that discordantly cross-cut metamorphic fabrics, constrain Kurgiakh deformation and metamorphism to be *c.* 484-473 Ma (Myrow *et al.* 2016; see also Gehrels *et al.* 2006). Metamorphic garnets also yield 29-25 Ma Th/Pb monazite ages attributed to a regional metamorphic overprint during Cenozoic tectonic loading (Gehrels *et al.* 2006). Metamorphic grades vary from kyanite to no higher than biotite facies from north to south, respectively, across the area (Cawood *et al.* 2007). Our samples include three foliated marbles from the Bhimpihedi Group in the south and one Phulchauki Group limestone from the Godavari quarry in the central part of the klippe (Pas *et al.* 2011) (Fig. 6c-e). Two of the three Neoproterozoic samples (BEi and MU2) have maximum shortening axes that lie off the bedding great circle (LNS: Fig. 18). Both samples show single compression axis maxima, indicating a simple twinning record. The third sample (MUI) has a maximum shortening axis that lies near the bedding great circle (LPS) but shows bimodal compression axis maxima, indicating a complex twinning history. The Silurian sample (GQI) yielded high negative expected values (40%) indicating non-coaxial twinning strains. Positive expected values yield a maximum shortening axis that lies within the compression axis maxima near the bedding great circle (LPS), whereas negative expected values yield a maximum shortening axis that lies within the compression axis maxima at a high angle to bedding (LNS).

Tibet

The upper Neoproterozoic-Cambrian Rouquicun Group in the Nyalam area of the Tibetan Himalaya (Fig. 5) includes foliated Cambrian quartzite, psammitic schist and marble (Fig. 6g) that stratigraphically correlate with the upper Neoproterozoic-Cambrian Haimanta Group in the Spiti and Zanskar areas of the Indian Himalaya (Myrow *et al.* 2009). To the northofNyalam, theRouquicun

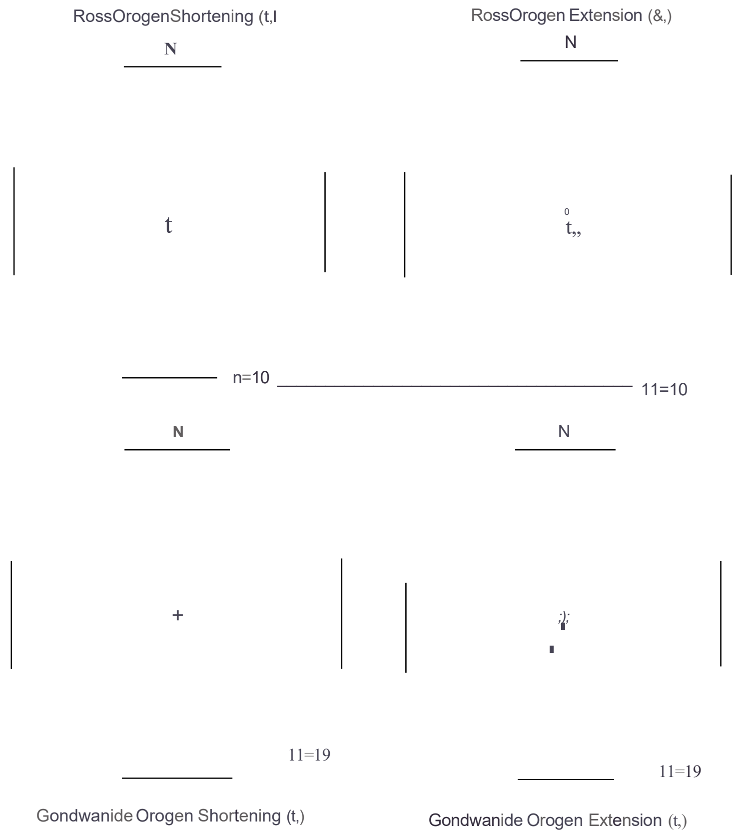

Fig. 12. Lower-hemisphere stereonet plots of shortening *(e_1)* and extension axes (e_3) for (upper) the Ross (Ordovician) and (lower) Gondwanide (Permian) orogens in the Cape Fold Bell, South Africa. The tectonic transport direction is to the north. Key: (upper) filled circle, limestone; open circle, vein; open square, vein NEV; (lower) filled diamond, foreland (limestone and vein); filled circle, limestone or quartzite; open circle, vein; open square, vein NEV.

Group is juxtaposed against unmetamorphosed Ordovician limestone of the Chiatsum Group, which post-dates the Kurgiakh Orogeny and presently occupies the hanging wallof the South Tibetan Detachment System (STDS: Fig. 6h), a major Cenozoic down-to-the-north normal fault (Burchiel *et al.* 1992; Wang *et al.* 2006). Cambrian rocksof the Rouquicun Group were metamorphosed and deformed during Cenozoic tectonic burial and shearing along the STDS (Wang *et al.* 2015). We nevertheless analysed a sample of Rouquicun Group marble, given the evidence that some metamorphism within the Greater Himalaya is likely to have occurred earlier during the Kurgiakh Orogeny (Gehrels *et al.* 2006). Our samples come from the area where Myrow *et al.* (2009) reported Cambrian detrital zircon ages from the Rouquicun Group and include three unmetamorphosed Ordovician limestone samples from the hanging wall of the STDS, as well as a Permian limestone from an area north of Mount Everest/Chomolungma. The Cambrian and Ordovician rocks stratigraphically correlate with the North Col Formation and Ordovician rocks on Mount Everest/Chomolungma (Myrow *et al.* 2009). The Cambrian sample (N8) and two of the Ordovician samples (N20 and N21) yield maximum shortening axes that lie at a high angle to the bedding great circles (LNS: Fig. 18). The other Ordovician sample (NI9) and Permian sample (N34) yield maximum shortening axes that lie near to the bedding great circles (LPS). All but one of the samples (Nl9) show single compression axis maxima that generally coincide with the maximum shortening axes, indicating simple twinning records; N19 shows a maximum shortening axis that lies away from the compression axis maxima, suggesting a more complex twinning record.

Bhutan

Rocks within klippe in theBhutan Himalaya (Fig. 5) include Cambrian-Jurassic strata that have been

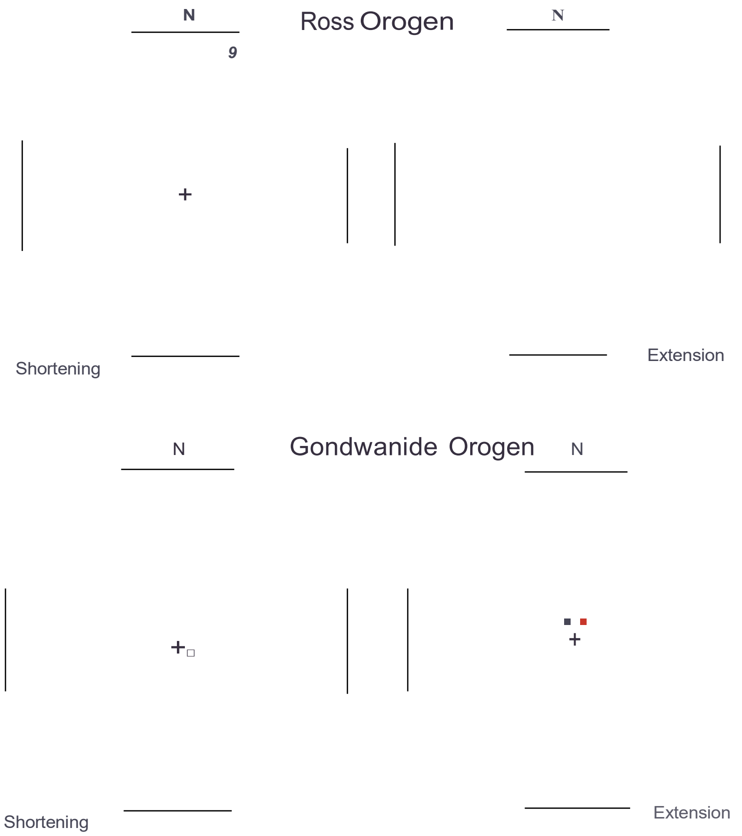

Fig. 13. Lower-hemisphere projections of (left) shortening and (right) extension axes for calcite twinning strain data from the Heritage Range, Ellsworth Mountains, Antarctica (see Table 2) (see Craddock *et aL* 2017b). Key: filled circle, limestone; open circle, vein; red circle, limestone (NEV); open square, vein (NEV).

emplaced on metamorphic rocks of the Greater Himalaya by north-directed movement along the STDS (Long *et al.* 2011). Our samples come from the Tang Chu Klippe (Hughes *et al.* 2011) and include one recrystallized Cambrian limestone that predates the Kurgiakh Orogeny. We also analysed two recrystallized Ordovician-Silurian limestone samples of theWachi La Formation, which post-date this orogeny (Fig. 6t). The Cambrian sample (273.74) and Ordovician-Silurian sample (PLJ) yield maximum shortening axes that lie near the beddinggreat circles (LPS: Fig.18). Both samples show single compression axis maxima indicating a simple twinning record. Sample WL9902 (Ordovician-Silurian) yielded high negative expected values (40%), indicating a non-coaxial twinning record. Separate analyses of positive and negative expected values yield maximum shortening axes that lie within the compression axis maxima near the bedding great circle (LPS), although the NEV population yields bimodal compression axis maxima that indicate a complex twinning history.

Discussion

Late Neoproterozoic-early Paleozoic deformation associated with the final assembly of Gondwana varied in both space and time. This deformation is preserved as a complicated pattern of shortening axes and fabrics (Figs19 & 20), a possible resultof spatio-temporal variations in stress regimes (Table 2) along the various convergent boundaries involved in the construction of Gondwana. Early Paleozoic differential stress magnitudes are low, soprojecting regional stress-strain fields over the timespan of the orogeny is speculative (Fig. 21). The classic Gondwana sedimentary sequence (du Toil 1937;Frakesand Crowell 1967, 1969; Crowell 1978; Craddock 1982; Craddock *et al.* 2019a) was deformed during the late Paleozoic along a convergent, then dextral, transcurrent margin that was coeval with the Gondwana-Laurussia collision, recorded as the Variscan-Alleghenian-Atlas orogen. Gondwanide orogen differential stresses were higher than Ross orogen stresses, and the Gondwanide orogen is dominated

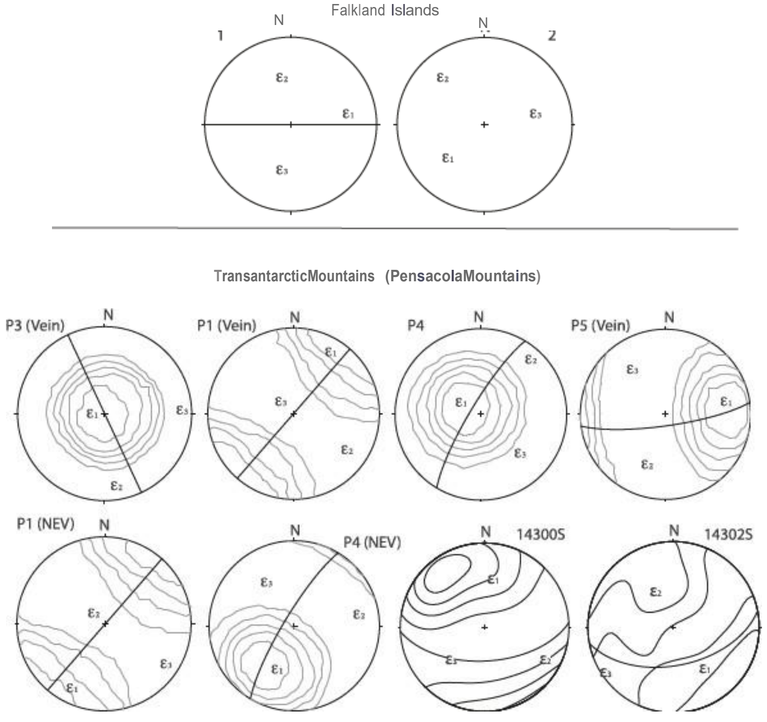

Fig. 14. Lower-hemisphere projections of (upper) finite-strain (Falkland Islands) and (lower) calcite-strain (Cambrian Nelson Limestone and veins, Pensacola Mountains) data.See Table 2. Key: great circles are bedding or vein orientations; ε_1, shortening axis; ε_2, intermediate axis; ε_3, extension axis.

by LPS fabrics that can be projected from plate boundary to plate boundary across Pangaea (Fig. 22).

Early Paleozoic orogenic patterns

Most of the sample sites from early Paleozoic orogenic belts lack a contemporaneous, stable cratonic strain site to compare to allochthonous rocks in the adjacent orogenic belt (see below), so our local tectonic transport direction plots (Fig. 20) are referenced to fold axes and fault kinematic data. The *c.* 540 Ma Ribiera orogen represents the oldest sample site within our dataset and is the only site from interior Gondwana. The calcite in these high-grade calc-silicates preserves horizontal shortening strain normal to the ENE-trending local margin and parallel to the fault kinematic vectors, with horizontal extension parallel to the inferred margin (Fig. 20b).

Along Gondwana's southern margin, twinning fabrics are more complicated (Fig. 20c), and may reflect poorly understood temporal changes in shortening intensities and directions associated with

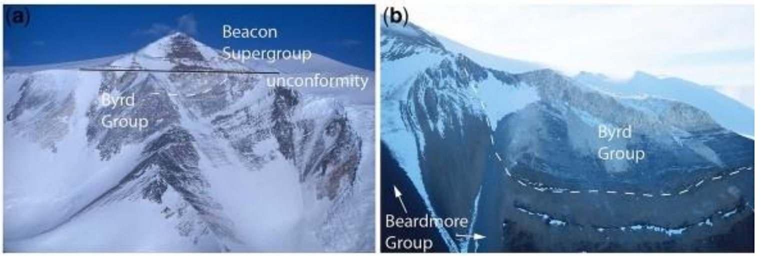

Fig. 15. Field photographs showing Ross deformation. (a) Angular unconformity separating deformed Shackleton Limetone (Byrd Group; below) and the overlying undeformed Devonian-Jurassic Beacon Supergroup in the central Transantarctic Mountains. **(b)** Syncline of Shackleton Limestone (Byrd Group) overlying the dark-coloured Beardmore Group at the Palisades in the Nimrod Glacier area.

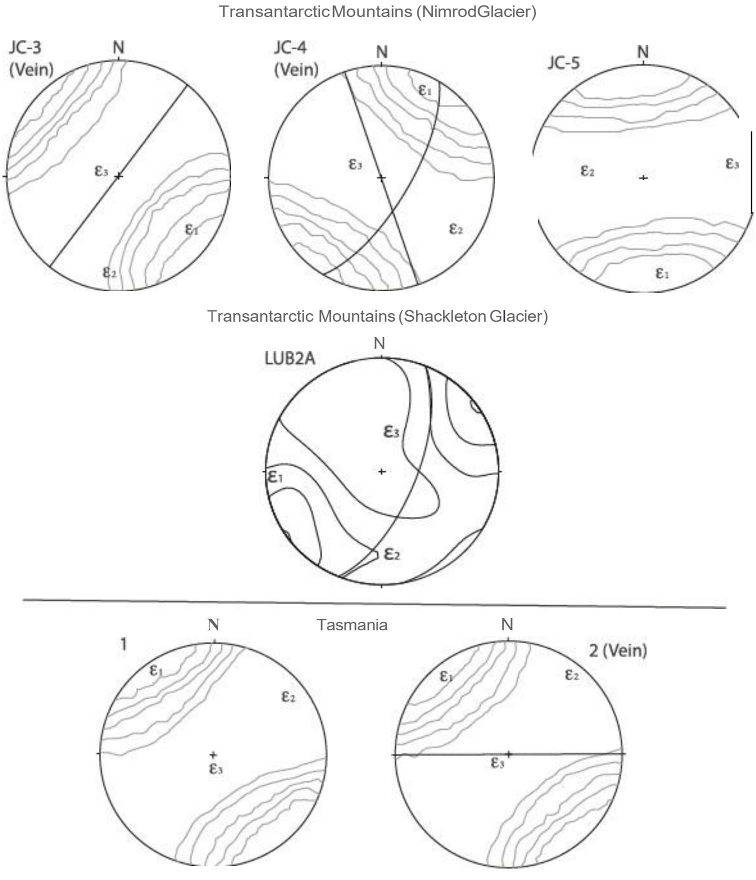

Fig. 16. Lower-hemisphere projections of calcite strain data (see Table 2) for (upper) the Transantarctic Mountains, Antarctica and (lower) Maria Island, Tasmania. Key: great circles are bedding or vein orientations; e_1, shortening axis; e_2, intermediate axis; ε_3, extension axis.

accretionary orogenesis along the Ross belt. Ross orogen deformation and metamorphism has been shown to have initiated by *c.* 590-570 Ma in South Victoria Land in Antarctica (Hagen-Peter *et al.* 2016). However, Cambrian sedimentary successions show markedly different degrees of deformation from west to east along this margin. The deformation of Cambrian limestone in South Africa, the Ellsworth Mountains and the Pensacola Mountains is weak to absent, whereas strongly folded and faulted Cambrian limestone in the Transantarctic Mountains in Antarctica have long been considered the hallmark of the Ross Orogeny.

In South Africa, the Saldanian Orogeny constitutes the main phase of deformation. Rocks deformed during the Saldanian event are unconformably overlain by basal sandstone of the Ordovician Table Mountain Group (Barnett *et al.* 1997; Armstrong *et al.* 1998). Detrital zircon analyses from the Table Mountain Group suggest that the main phase of Saldanian deformation occurred before 520 Ma, and was followed by deposition of pre-Table Mountain Cambrian successions in post-orogenic rift basins along the margin (Armstrong *et al.* 1998). Cambrian limestones and veins in the Kango Inlier, which sits structurally and stratigraphically below the Paleozoic Cape Supergroup and appears to have been little deformed during the late Paleozoic Cape Fold Belt Orogeny, present a challenging interpretation. All the Kango samples are from the same outcrop belt, so there are two deformational interpretations: (1) the Cambrian limestone may have been deposited in a half-graben then slumped to a vertical east-west orientation, subsequently experienced Ross orogen north-south horizontal shortening but remained unaffected by Gondwanide orogen deformation, including clockwise rotation and nappe stacking (no vertical twinning strain overprint except for sample Kango--6; see Craddock *et al.* 2007b, 2017b); or (2) the

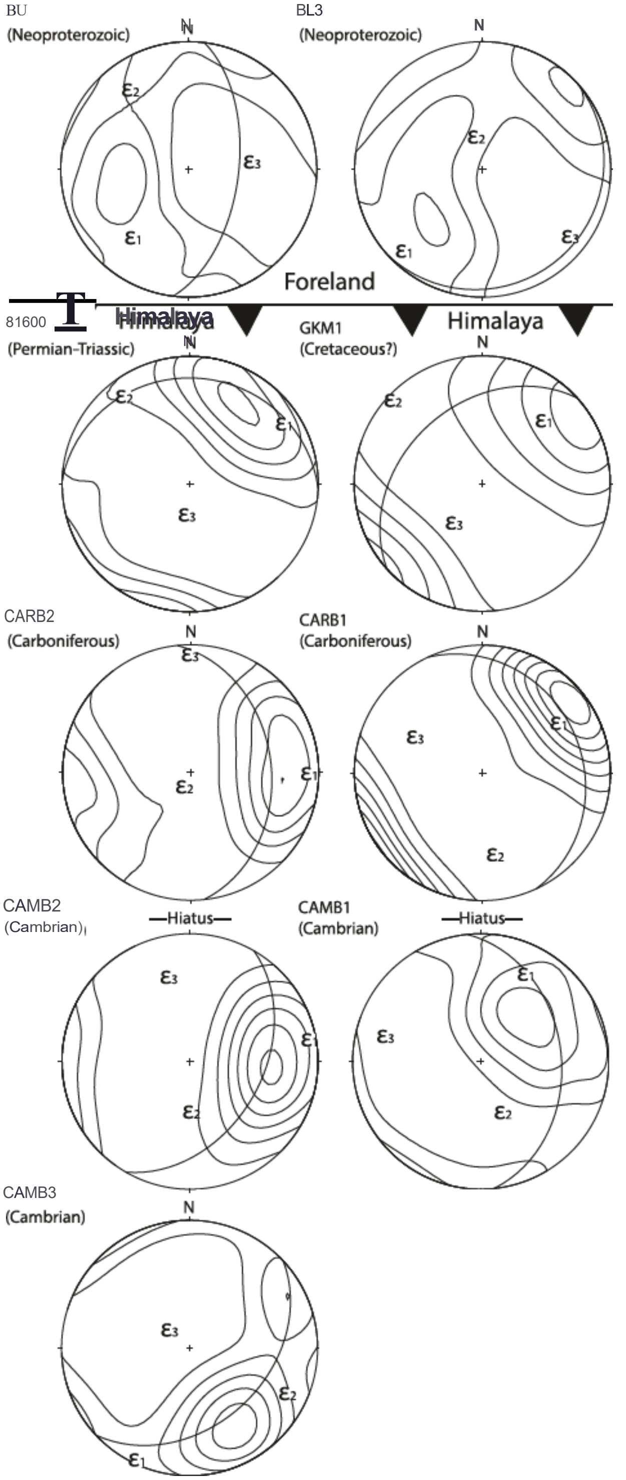

Fig. 17. Lower-hemisphere projections of calcite strain data from India (see Table 2). 'Hiatus' marks the relative location of the unconformity associated with the Kurgiakh Orogeny.

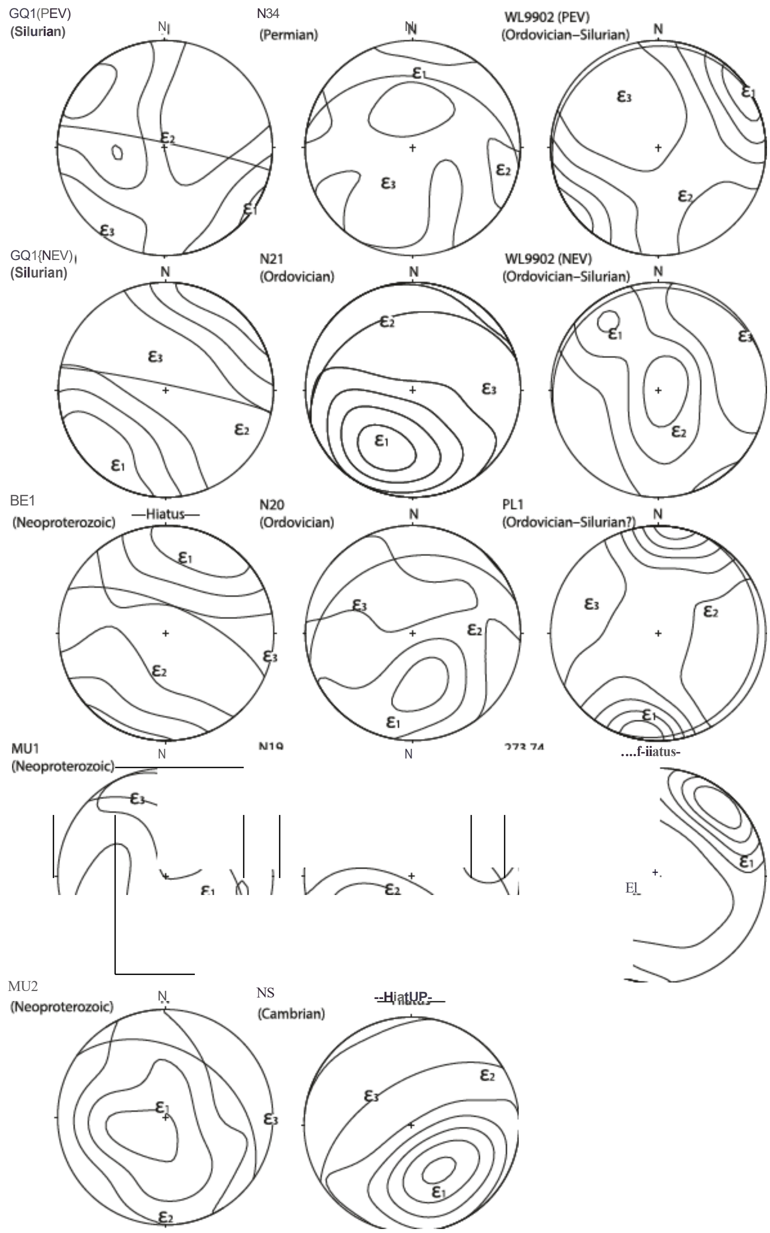

Fig. 18. Lower-hemisphere projections of calcite strain data from Nepal, Tibet and Bhulan (see Table 2). 'Hiatus' marks the relative location of the unconformity associated with the Kurgiakh Orogeny.

Cambrian limestone was deposited in a half-graben, remained undeformed until the end of the Permian and was then rotated to vertical and deformed by north-south horizontal Gondwanide shortening, again without clockwise rotation or any nappe-related vertical shortening overprint (except for sample Kango-6).

In the Ellsworth Mountains, early mapping has indicated that Cambrian deformation was weak (Craddock 1969), and that the main phase of deformation was related to NW-trending folding associated with the upper Paleozoic Gondwanide orogen. Duebendorfer and Rees(1998)argued thatCambrian deformation is expressed as an angularunconformity

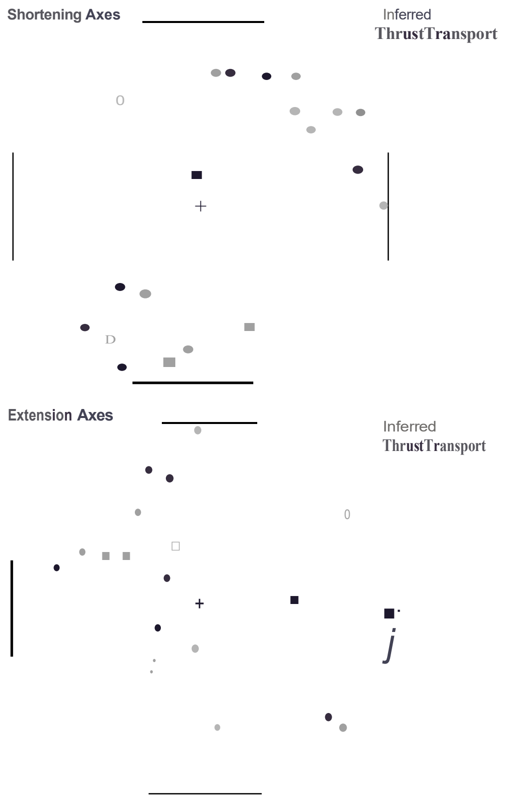

Fig. 19. Lower-hemisphere projections of strain data (upper: shortening axes; lower: extension axes) (see Table 2) for twinning data by fabric interpretation of rocks involved in the Cenozoic Himalayan orogen (and foreland; $n = 13$; grey symbols) and the ancestral late Cambrian-early Ordovician Kurgiakh orogen ($n = 10$; black symbols). Key: filled circle, LPS; open circle, LPS (NEV); filled square, LNS, open square, LNS (NEV).

separating Cambrian and Ordovician rocks, as well as by local refolded folds and a crenulation cleavage. However, other authors have rejected this idea and have,instead, argued that Rossdeformation is absent and that Cambrian deposition occurred in a continental rift basin along the margin (Curtis 2001). There are no strain data for Devonian-Pennian Gondwana strata overlying theCambrian-Ordovicianunconformity. However, our data from the Cambrian section suggest shortening at a high angle to NW-trending folds and axial-planar cleavages found in the Gondwana succession, suggesting that the twinning fabrics may reflect Gondwanide shortening (Craddock et al. 2017c) or an earlier coaxial Cambrian shortening event; a possibility that is consistent with Type 3 fold interference patterns reported from Cambrian rocks in the area (Duebendorfer and Rees 1998).

In the Pensacola Mountains, the main phase of early Paleozoic deformation associated with the Ross Orogeny occurred prior to deposition of the late middle Cambrian Nelson Limestone, which unconformably overlies highly deformed late Neoproterozoic-Cambrian greywacke of the Hannah Ridge Formation (Curtis et al. 2004). These rocks were folded during the late Paleozoic Gondwanide Orogeny but stratigraphic and structural relationships suggest an earlier coaxial shortening episode characterized bygentle late Cambrian-early Ordovician folding of the Nelson Limestone at shallow depths during the tenninal stages of the Ross Orogeny (Storey et al. 1996). Our strain data from two Nelson Limestone samples are consistent with LPS orientated at a high angle to the active margin, whereas strains from veins record shortening subparallel to NE-trending folds. The origin of this shortening strain is unknown but could be related to Cambrian orogenesis associated with the closure of the Mozambique Ocean recorded in the Shackleton Range c. 500 km NE of the Pensacola Mountains (Buggisch and Kleinschmidt 2007).

In the Transantarctic Mountains, early Paleozoic deformation is well expressed by folds and cleavage within Cambrian limestones that are locally metamorphosed and cross-cut by syn- to post-tectonic granitoids (Myrow et al. 2002; Goodge et al. 2004a, b; Paulsen et al. 2007b). The calcite strain data preserve a LNS strain at a high angle to the local structural grain in the Shackleton Glacier area (Paulsen et al. 2004). Data from the Nimrod Glacier area record a mix of shortening strains that areorientated oblique the local NNW trend of folds (Table 2; Fig.20). One vein collected c. 100 km to the west in the Miller and Geologists ranges, where deformation involved a margin-parallel component of displacement, records NW-shortening consistent with top-to-the SE ductile shear fabrics older than 515 Ma (Goodge et al. 1993). The north- to NNE-shortening strains recorded in the other Nimrod Glacier samples are consistent with east-trending folds located c. 200 km north of our sample sites on the south side of Byrd Glacier.

Along Gondwana's northern margin, Cambrian limestone preserves a mix of LPS and LNS fabrics that plot in a crude NE-SW-orientated, margin-normal girdle (Fig. 19). Our Indian Himalaya samples yield NE-SW to east-west LPS fabrics that are roughly parallel to LPS fabrics in Ediacaran limestone on the Indian Shield, as well as in Carboniferous-Cretaceous carbonate of the Himalayan orogen (Fig. 17), consistent with coaxial shortening implied by parallel early Paleozoic and Cenozoic fold axes found in this sector of the Himalaya (Dezes 1999; Wiesmayr and Grasemann 2002). The diagenetic to low-epizone grade of metamorphism of the Cambrian successions at these localities (Wiesmayr and

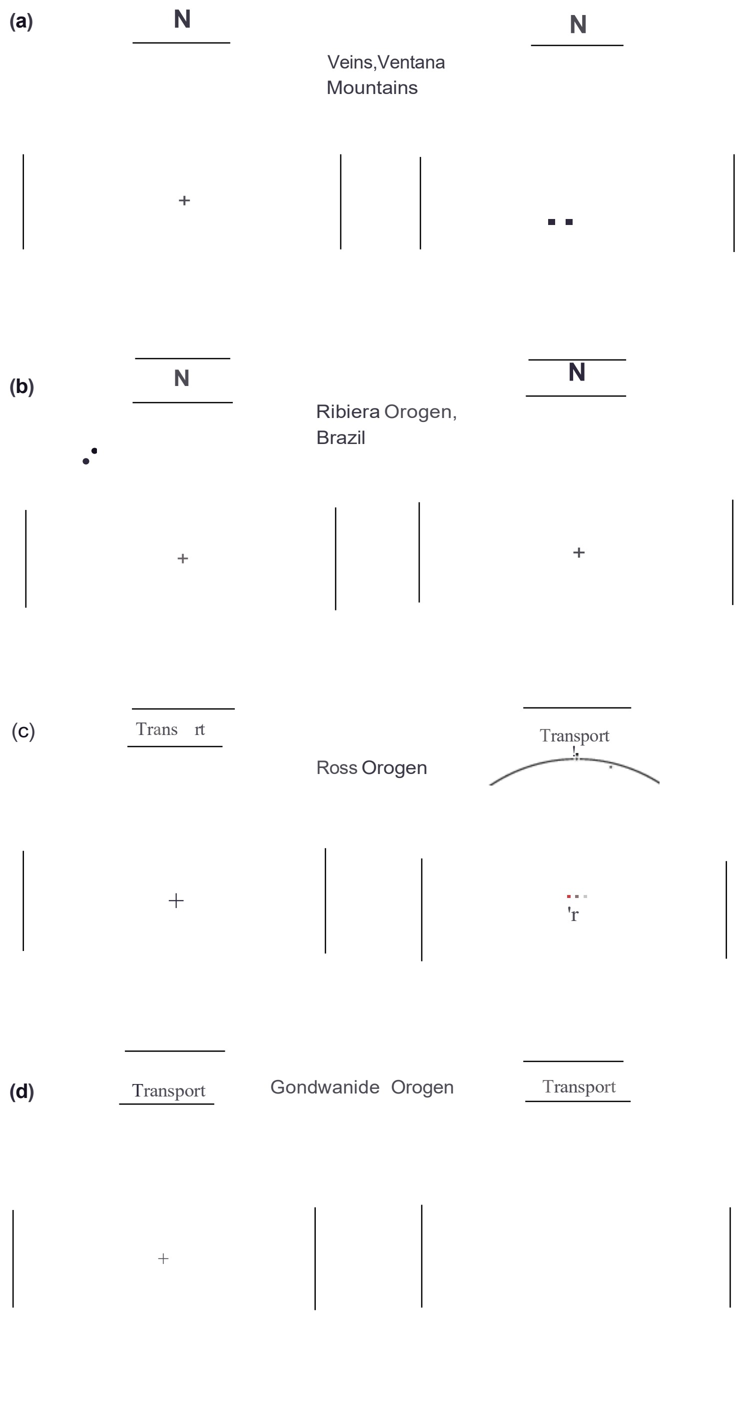

Fig. 20. Lower-hemisphere projections of strain data (fable 2) for: (a) anomalous calcite veins in the Ventana Mountains, Argentina; (b) calc-silicates in the 540 Ma Ribiera orogen, Brazil; (c) the early Ordovician Ross orogen; and (d) the Permian Gondwanideorogen. Key: (left) shortening axes; (right) extension axes. Plotted symbols: filled diamond, foreland; filled circle, LS or quartzite; open circle, vein; open square, vein (NEV); open red circle, LS (NEV).

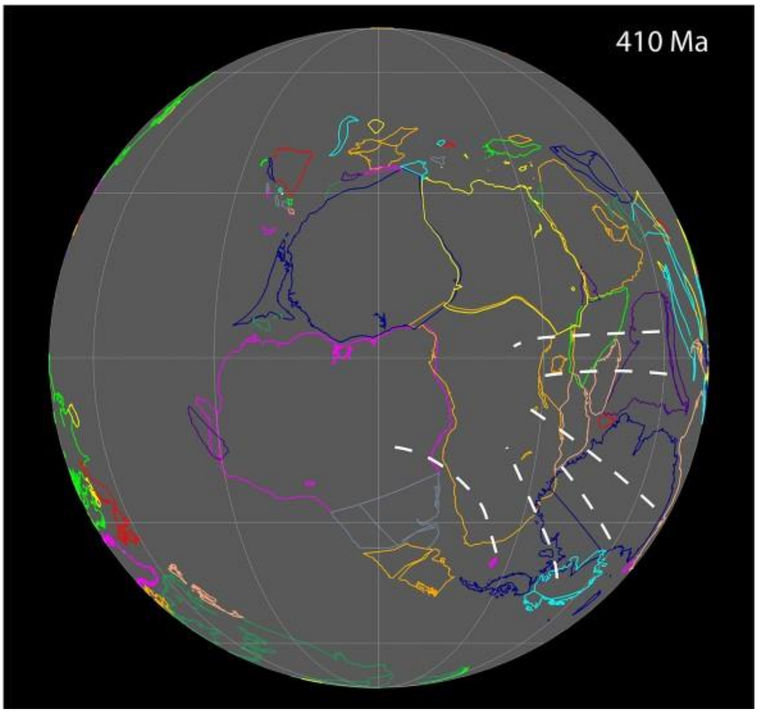

Fig. 21. Tectonic reconstructions of Gondwana following the Terra Australis (Ross: 410 Ma) orogen created by GP!ates (Millier *et al.* 2018). Strain shortening axes are plotted and projected inboard from the margin Ross (Terra Australis) tectonic summary.

Grasemann 2002) suggest that the strains in the Cambrian samples are primary and not overprinted by Himalayan deformation. Our Cambrian samples from areas to the east in the Himalaya show similar strains that are indistinguishable from Cenozoic Himalayan strains recorded in carbonate that post-dates the Kurgiakh Orogeny. Cambrian sedlmentary successions show markedly higher degrees of metamorphism to the east at our other Himalaya sample sites (Myrow *et al.* 2016). Metamorphism of Himalayan rocks is now recognized to be, at least in part, early Paleozoic in age (Gehrels *et al.* 2006; Palin *et al.* 2018). However, strains within some of our samples are likely to record a Himalayan strain overprint.

In Nepal, the NW-SELPSfabrics recorded in the Silurian GQI (PEV) and Neoproterozoic MUI samples(Fig. 18) trend sub-parallel to NW-SE-trending Cenozoic fold axes in the Kathmandu Klippe (Gehrels *et al.* 2006). These LPS fabrics may record early layer-parallel shortening prior to folding but are also consistent with Cenozoic range-parallel shortening indicated by transverse folding elsewhere in the orogen (Johnson 1994; Long *et al.* 2011). The shallow NE-SW LNS strains recorded in the GQI (NEV) and Neoproterozoic BEl samples trend at a high angle to the NW-SE Cenozoic fold axes, as well as a steep NW-SE spaced cleavage that truncates fossil fragments within the GQ1 sample. These relationships are consistent with twinning due to syn- to post-folding horizontal shortening in these areas. The steep LNS strain recorded in the Neoproterozoic MU2 sample could reflect later tectonic rotation of the syn- to post-folding horizontal shortening record in MUI;however, it is also consistent with twinning during post-folding lithostatic loading due to tectonic or sedimentary burial.

In Tibet, twinning strains recorded in thefootwall (metamorphosed) and hanging wall (unmetamorphosed) of the SIDS are different (Fig. 18). The LNS fabric recorded in the metamorphic rocks in the footwall of the STDS by Cambrian sample NS is at a high angle to metamorphic foliation. Twinning within sample NS also records a layer-parallelextensional strain. This relation suggests that twinning may record Cenozoic extension along the detachment. Twinning fabrics recorded in the hanging wall of the SIDS by Ordovician samples N19-21 also yield NW-SE maximum extensional strains. However, the LNS fabrics recorded with these

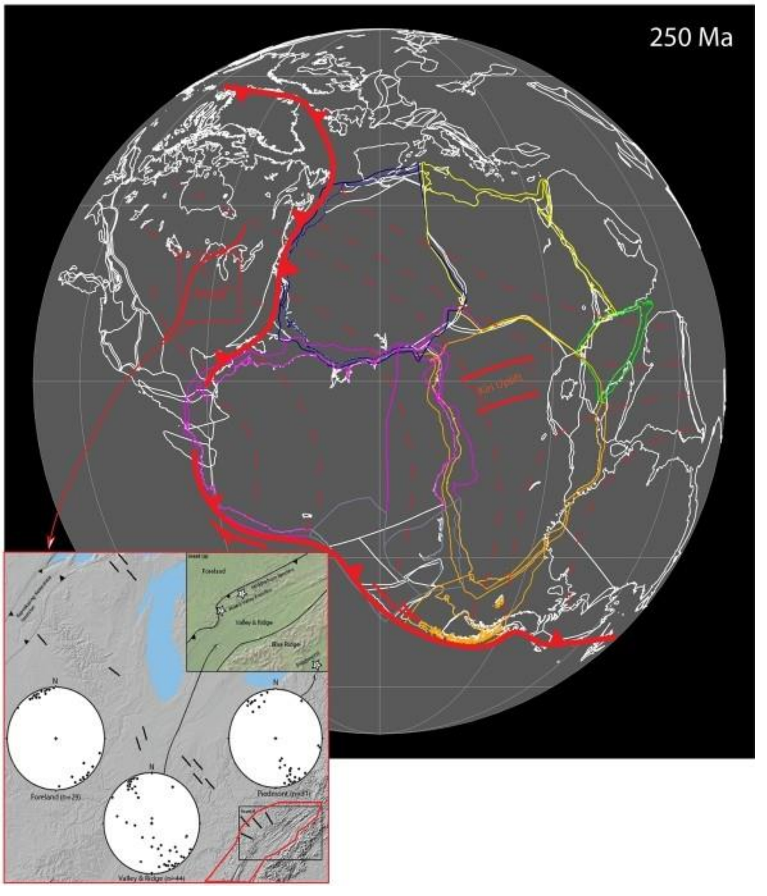

Fig. 22. GPLATES reconstruction of Pangea at *c.*250 Ma showing the margin-normal shortening strains of the Alleghenian-Atlas orogen (north: see inset a from Craddock and Malone 2021) and the shortening strain field continuum across Africa and South America to the dextral boundary on the southern margin of Gondwana.

samples trend at a high angle to SW-vergent, WNW-ESE-trending Cenozoicfold axes within theTethyan fold-thrust belt (Burchiel *et al.* 1992; Wang *et al.* 2015). Collectively, these relationships may reflect fold-parallel extension with shortening at an oblique angle to bedding due to frictional resistance along a basal thrust or hanging-wall bending strains associated with footwall ramps (Evans and Dunne 1991) that are associated with SW direction thrusting. The north-south LPS fabric recorded in the N34 sample trends at a high angle to the Cenozoic fold axes in the Tethyan fold-thrust belt, consistent with early layer-parallel shortening prior toCenozoic folding.

In Bhutan, Cambrian and Ordovician-Silurian samples record roughly parallel NE-SWLPSfabrics (Fig. 18), consistent with coaxial early Paleozoic and Cenozoic shortening or, alternatively, with a Cenozoic overprint recorded in the older sample. The NW-SE LPS strain recorded in sample WL9902 (NEV) trends at an oblique angle to the dominant east-west trend of Cenozoic folds in Bhutan but is consistent with range-parallel shortening expressed by transverse NE-SW folding in the area (Long *et al.* 2011).

Gondwanide orogen

The Gondwanide orogen extends for 2500 km through the Ventana Mountains (west), the Cape Belt, Falkland Islands, Ellsworth Mountains and Tasmania (Figs 1, 3 &4). Thisthin-skmned belt includes craton-vergent, asymmetrical folds with an axial-planar cleavage and 30-50% shortening along thrust faults (Fig.7) (Halbich and Swart 1983; de Wit 1992; Johnston 2000). We report strain results from twinned calcite ($n=34$; strain overprints are measured with this technique) and finite strains in quartzite samples ($n=15$; no strain overprints are measured with this technique), so characterizing the regional strain patterns mixes different methods. Craddock *et al.* (2007a) reported north-south horizontal shortening LPS strain results from the southernmost Karoo Basin in flat-lying Permian limestone (triangle symbol in Fig. 18). We use this result as our reference for Gondwana shortening across the Cape Belt, which is very different from the synfolding, bedding-parallelcalcite filling in the nearby Permian Prince Albert Formation shale that records rotation of shortening strain axes to the east through the fold axes. The finite strains in quartzite samples all preserve a layer-parallelshortening strain thatis rotated clockwise from thestable LPS fabricin the foreland. The calcite strain patterns include results from limestone, veins and strain overprints preserved in both, all of which plot as a girdle *c.* 35° clockwise from the north-south horiwntal shortening preserved in the Karoo foreland; thus, supporting a dextral component of motion along the Gondwana margin to the south (Fig. 22).

Strain anomalies

Four vertical calcite veins were analysed in the Ventana Mountains in Argentina (Table 2). Three preserved an approximately north-south horizontal shortening strain fabric (with vertical extension), and thefourth, a horizontalvein, recorded verticalshortening (and east-west extension). None of these veins is dated nor are the strain results similar with any other Gondwanide orogen strains, so perhaps these were veins associated with the Andean orogen (Ramos 1988a, *b;* Fig.22).

Pangaea

Daly *et al.* (1991) were the first to identify a mid-crustal inversion structure - the Kiri uplift - in the centre of a supercontinent (i.e. Gondwana), which offset Permian strata that are overlain by flat-lying Cretaceous rocks, suggesting a far-field structural response to a deformation somewhere along the margin of Africa. Craddock *etal.* (2017b) proposed that this Permian pop-up structure was the result of far-field shortening associated with north-south horizontal Gondwana orogen shortening from the south, SE-directed shortening from the Alleghenian-Atlas collision to the NE or both (Fig. 22). The contribution of horizontal shortening from the Africa-India margin from the east is less clear but curvilinear, horizontal, stress-strain fields are projected across central Africa. The Gondwana orogen differential stress magnitudes were higher (Table 2) than Rossorogen stresses, contributing, with thecollisional Alleghenian-Atlas orogen, to the propagation of tectonic stress across Gondwana into Laurussian in the Permian.

Conclusions

Strain patterns along the southern early Paleowic Gondwana margin are complex, with a wide array of shortening axes, strain fabrics (LPS, LNS, VNS and VPS) and local strain overprints. Tectonic interpretations are limited because there are no strain samples from the stable craton to record contemporaneousdeformation and a kinematic reference site; this indicates that Ross-related deformation was local and included intrusion of contemporaneous arc-related plutons.The collisional Buzios orogen preserves sub-horiwntal shortening strains parallel to the inferred collisional and tectonic transport direction, although, curiously, with many stacked nappes but no strain overprint. 1\vinning strains in Cambrian carbonates in the Himalaya preserve LPS fabrics parallel to the inferred thrust transport direction of the Kurgiakh orogen. Early Paleowic orogenesis along Gondwana's southern margin was regional and episodic, and it is difficult to argue for far-field effects.

The Permian Gondwanide orogen is characterized by a regional LPS fabric anddextral rotation of shortening axes along the southern Gondwana margin, whereas collisional orogens dominated the contemporaneous Appalachian-Caledonide margins as Pangaea amalgamated. Arc rocks are absent along the dextral Gondwana and the collisional Appalachian-Caledonide margins. Far-field effects of these contemporaneous orogens are supported by LPS fabrics 2000-3000 km inboard in foreland settings and crystalline-cored inversion of the Kiriuplift in central Africa and the Keweenaw-Kapuskasi ngupliftin central North America (Craddock and van der Pluijm 1989; Craddock *et al.* 1993, 2017a).

Acknowledgements J. Craddock and S.T. Johnston benefited from the organizational skills of Maarten de Wit at the excellent Gondwana 10 meeting in Cape Town in July 1998 and the fabulous post-meeting trip that Maarten led across theCape belt J. Craddock also had the pleasure of visiting the Ellsworth Mountains, Tasmania, the Cape, and the Ventana and Falkland portionsof the Gondwanide belt with Jeny Webers (deceased, 2008).John Goodge and Michael Reiser contributed the samples from the Nimrod Glacier area of the Transantarctic Mountains, and Mike Curtis (formerly of the British Antarctic Survey) contributed samples from the Pensacola Mountains. Macalester students Alex McKiernan and Carolyn Kilberg contributed to the Cape Belt strain measurements. Reviews by Dave Malone and Gabriel Gutierrez-Alonso are greatly appreciated.

Competing interests The authors declare that they have no known competing financial interests or personal relationships that could have appeared to influence the work reported in this paper.

Author contributions JC: conceptualization (lead), datacuration (lead), investigation (lead), writing - original draft (lead), writing - review & editing (lead); **TP:** conceptualization (equal), data curation (equal), writing - review & editing (equal); **ROSS:** conceptualization (equal), data curation (equal), writing - review & editing (equal); **STJ:** conceptualization (equal), data curation (equal), writing - review & editing (equal); **PMM:** writing- review & editing (equal); **NCH:** writing - review & editing (equal).

Funding Portionsofthisworkwerefunded by the United StatesScience Foundation (grant No. NSF EAR-1849963) andIGCP668, aswell asa University of Wisconsin Oshkosh Faculty Development Program to T. Paulsen.

Data availability Data are available from John Craddock.

References

Alessandretti, L., Philipp, R.P., Cbemale, F., Jr,Briickmann, **M.P.**, Zvirtes, **M.,** Matte, V. and Ramos, **V.A.** 2013. Provenance, volcanic record, and tectonic setting of the Paleozoic Ventania Fold Belt and the Claromec6 Foreland Basin: Implications on sedimentation and volcanism along the southwestemGondwanamargin.*South AmericanJournalofEarthSciences,* 47, 12-31, https://doi.org/ 10.1016/j.jsames.2013.05.006

Armstrong, **R.,** de Witt, **M.J.,** Reid, D., York, D. and Zartman, R. 1998. Cape Town's Table Mountain reveals rapid Pan African uplift of its basement rocks. *Journal of African Earth Sciences,* 27, 1 11.

Barnett, W., Armstrong, R.A. and de Wit, M.J. 1997. Stratigraphy of the upper Neoproterozoic Kango and lower Palaeozoic Table Mountain Groups of the Cape Fold Belt revisited. *South African Journal of Geology,* 100, 237-250.

Boger, S.D. 201I. Antarctica-before and afterGondwana *GondwanaResearch,* 19, 335-371, https://doi.org/10.1016/j.gr.2010.09.003

Boger, S.D. and Miller, J.M. 2004. Terminal suturing of Gondwana and the onsetof the Ross-Delamerian Orogeny: thecause andeffectof an EarlyCambrian reconfiguration of plate motions. *Earth and Planetary Science Letters,* **219,** 35-48, https://doi.org/10.1016/S0012-821X(03)00692-7

Buggisch, W. 1987. Stratigraphy and very low-grade metamorphism of the Sierras Australes de la Provincia de Buenos Aires (Argentina) and implications in Gondwana correlation. *7.entralblan Mineralogie Geologie Pali:iontologie,* 1, 819-837.

Buggisch, W. and Kleinschmidt, G. 2007. *The Pan-African Nappe Tectonics in the Shackleton Range.* USGS Open-File Report, 2007-1047, Short Research Paper 058, https://doi.org/10.3133/of2007-1047.srp058

Burchiel, B.C., Chen, Z., Hodges, K.V., Liu, Y., Royden, L.H., Deng, C. and Xu, J. 1992. The *South Tibetan Detatchment System, Himalayan Orogen: Extension Contemporaneous with and Parallel to Shortening in a Collisional Mountain Belt.* Geological Society of America Special Papers, 269.

Burkhard, M. 1993. Calcite twins, their geometry, appearance and significance as stress-strain markers and indicators of tectonic regime: a review. *Journal of Structural Geology,* **15,** 351-368, https://doi.org/10.I016/0191-8141(93)90132-T

Cawood, P.A. 2005. Terra Australis Orogen: Rodinia breakup and development of the Pacific and lapetus margins of Gondwana during the Neoproterozoic and Paleozoic. *Earth-Science Reviews,* 69, 249-279, https://doi.org/10.1016/j.earscirev.2004.09.001

Cawood, P.A. and Buchan, C. 2007. Linking accretionary processes with supercontinent assembly. *Earth-Science Reviews,* 82, 217-256, https://doi.org/ IQ.I016/j.earscirev.2007.03.003

Cawood, P.A., Johnson, M.R.W. and Nemchin, A.A.2007. Early Paleozoic orogenesis along the Indian margin of Gondwana: tectonic response to Gondwana assembly. *Earth and Planetary Science Letters,* 255, 7 84, https:// doi.org/10.1016/j.epsl.2006.12.006

Cawood, P.A., Martin, E.L., Murphy, J.B. and Pisarevsky, S.A 2021. Gondwana's interlinked peripheral margins. *Earth and Planetary Science Letters,* 568, 117057, https:// doi.org/10.1016/j.epsl.2021.117057

Cbakraborty, P.P., Sharma, R. and Kumar, P. 2019. Earthquake-induced soft sediment deformation (SSD) structures from the Bilaralimestone formation, Marwar basin, India *Journal of Earth System Science,* **128,** 162, https://doi.org/10.1007/s12040-019-1182-x

Cobbold, P.R., Gapais, D. and Rossello, E.A. 1991. Partitioning of transpressive motions within a sigmoidal foldbelt the Variscan Sierras Australes, Argentina *Journal of Structural Geology,* 13, 743--758, https:/ / doi.org/ 10.1016/0191-8141(91)90001-Y

Craddock, C. 1969. Geology of the Ellsworth Mountains. *In:* Bushnell, V.C. and Craddock, C. (eds) *Geologic Maps of Antarctica.* American Geographical Society Antarctic Map Folio Series, **12,** plate ***N.***

Craddock, C. 1970. Tectonic map of Gondwana *In:* Bushnell, V.C. and Craddock, C. (eds) *Geologic Maps of Antarctica.* American Geographical Society Antarctic Map Folio Series, **12,** plate **XXlll.**

Craddock, C. 1982. Antarctica and Gondwana: a review. *In:* Craddock, C. (ed.) *Antarctic Geoscience.* University of Wisconsin Press, Madison, WI, 3--14.

Craddock, C. and Webers, G.F.1964. Fossils from the Ellsworth Mountains, Antarctica. *Nature,* **201,** 174-175, https://doi.org/10.1038/201I74b0

Craddock, C., Bastien, T.W., Rutford, R.H. and Anderson, J.J. 1965. *Glossopteris* discovered in West Antarctica. *Science,* **148,** 634--637, https://doi.org/10.1126/science.148.3670.634

Craddock, C., Sporli, K.B. and Anderson, J.J. 1992. Structure of the Sentinel Range, Ellsworth Mountains, West Antarctica; Geology and paleontology of the Ellsworth Mountains, West Antarctica *Geological Society of America Memoirs,* 170, 393-402, https://doi.org/10.1130/MEM170-p393

Craddock, J.P. and Malone, D.H. 2021. An overview of strains in the Sevier thin-skinned thrust belt, Idaho and Wyoming, USA (latitude 42° N). *Geological Society of America Special Papers,* 555, 1-16, https://doi.org/10.1130/2021.2555(05)

Craddock, J.P.and McKiernan, A.W.2007.Tectonic implications of finite strain variations in Baraboo-interval quartzite.s(ca. 1700 Ma), Mazatzal orogen, Wisconsin and Minnesota, USA. *Precambrian Research,* 156, 175-194, https:// doi.org/ 10.1016/j.precamres.2006.03.010

Craddock, J.P.and Pearson, A. 1994. Non-coaxialhorizontal shortening strains preserved in amygdule calcite, DSDP Hole 433C, Suiko Searnount. *Journal of Structural Geology,* **16**, 719-724, hnps://doi.org/10.1016/0191-8141(94)90121-X

Craddock, J.P. and van der Pluijm, B. 1988. Kinematic analysis of an en echelon-continuous vein complex. *Journal of Structural Geology,* **10**, 445--452, hnps://doi.org/10.1016/0191-8141(88)90032-6

Craddock, J.P. and van derPluijm, B.A. 1989. Late Paleozoic deformation of the cratonic carbonate cover of eastern North America. *Geology,* **17**, 416--419, hnps://doi.org/10.1130/0091-7613(1989)017<0416:LPDOTC>2.3.CO;2

Craddock,J.P., Jackson, M, vander Pluijm, B.A.and Versical, R. 1993. Regional shortening fabrics in eastern North America: Far-field stress transmission from the Appalachian-Ouachita orogenic belt *Tectonics,* **12**, 257-264, https://doi.org/ 10.1029/92TC01I06

Craddock, J.P., Pearson, A., McGovern, M., Kropf, E.P., Moshoian, A. and Donnelly, K. 1997. Post-extension shortening strains preserved in calcites of the Keweenawan rift *Geological Society of America Special Papers,* **213**, 115-126.

Craddock, J.P., Neilson, K.J. and Malone, D.H. 2000. Calcite twinning strain constraints on Heart Mountain detachment kinematics, Wyoming. *Journal of Structural Geology,* 22, 983--991, https://doi.org/10.I0I6/S0I9 I-8141(00)00017-l

Craddock, J.P., Farris, D. and Roberson, A. 2004. Calcite-twinning constraints on stress-strain fields along the Mid-Atlantic Ridge, Iceland. *Geology,* 32, 49-52, https://doi.org/10.1130/GJ9905.1

Craddock, J.P., Anziano, J., Wirth, K.R., Vervoort, J.D., Singer, B. and Zhang, X. *2007a.* Structure, geochemistry and geochronology of a lamprophyre dike swarm, Archean Wawa terrane, Michigan, USA. *Precambrian Research,* 157, 5 70, https://doi.org/10.1016/j.precamres.2007.02.0 IO

Craddock, J.P., McKiernan, A. and DeWit, M.*2007b.*Calcite twin analysis in synorogenic calcite, Cape Fold Belt implications for fold rotation and cleavage formation. *Journal of Structural Geology,* 27, 11 1113, hnps://doi.org/ IO.1016 /j.jsg.2007.03.013

Craddock, J.P., Geary, J. and Malone, D.H. 2012. Vertical injectites of detachment carbonate ultracataclasite at White Mountain, Heart Mountain detachment, Wyoming. *Geology,* 40, 463--466, hnps://doi.org/10.1130/G32734.1

Craddock, J.P.,Craddock, S.D., Konstantinou, A., Kylander-Clark, A. and Malone, D.H. 2017a. Calcite twinning strain variations across the Proterozoic Grenville Orogen and Keweenaw-Kapuskasing inverted foreland, USA and Canada. *Geoscience Frontiers,* 8, 1357-1384, hnps://doi.org/10.1016/j.gsf.2017.01.006

Craddock, J.P., Fitzgerald, P., Konstantinou, A., Nereson, A. and Thomas, R.J. 2017b. Detrital zircon provenance of Upper Cambrian-Permian strata and tectonic evolution of the Ellsworth Mountains, West Antarctica. *GondwanaResearch,* 45, 191-207, hnps://doi.org/ IO.1016/j.gr.2016.11.011

Craddock, J.P., Schmitz, M.D. *et al. 2011c.* Precise U-Pb zircon ages and geochemistry of Jurassic granites, Ellsworth-Whitmore terrane, central Antarctica. *Geological Society of America Bulletin,* 129, 11S-136, https:// doi.org/10.113/B31485.l

Craddock, J.P., Malone, D.H. *et al. 2019a.*Calcite twinning strains from syn-faulting calcite gouge: Small-offset strike-slip, normal and thrustfaults. *International Journal of Earth Sciences,* **109**, 1--42, https://doi.org/10.1007/s00531-019-0J783-x

Craddock, J.P., Ojakangas, R.W. *et al. 2019b.* Detrital zircon provenance of Permo-Carboniferous glacial diamictites across Gondwana *Earth-Science Reviews,* **192**, 285-316, hnps:// doi.org/10.1016/j.earscirev.2019.01.014

Craddock,J.P., Nuriel, P., Kylander-Clark, A.R.C., Hacker, B.R., Luczaj, J. and Weinberger, R. 2022. Long-term (7 Ma) strain fluctuations within the Dead Sea transform from high-resolution U-Pb dating of a calcite vein. *Geological Society of America Bulletin,* **134**, 1231-1246, https://doi.org/ IO.I130/B36000.1

Crowell, J.C. I978. Gondwanan glaciation, cyclothems, continental positioning, and climate change. *American Journal of Science,* 278, 1345-1372, hnps://doi.org/10.2475/ajs.278.10.1345

Curtis, M.L. 1998. Development of kinematic partitioning within a pure-shear dominated dextral transpression zone: the southern Ellsworth Mountains, Antarctica. *Geological Society, LoTUWn, Special Publications,* 135, 289-306, hnps://doi.org/10.1144/GSL.SP.1998.135.01.19

Curtis, M.L. 2001.Tectonic history of theEllsworth Mountains, West Antarctica: reconciling a Gondwana enigma. *Geological Society of America Bulletin,* **113**, 939-958, https://doi.org/10.1130/0016-7606(200 I)11 3<0939:THOTFM>2.0.CO;2

Curtis, M.L., Leat, P.T., Riley, T.R., Storey, B.C., Millar, I.L. and Randall, D.E. 1999. Middle Cambrian rift-related volcanism in the Ellsworth Mountains, Antarctica: Tectonic implications for the palaeo-Pacific margin of Gondwana. *Tectonophysics,* **304**, 275-299, https://doi.org/10. IOL6/S0040-1951(99)00033-5

Curtis, M.L., Millar, I.L., Storey, B.C. and Fanning, M. 2004. Structural and geochronological constraints of early Ross orogenic deformation in the Pensacola Mountains, Antarctica. *Geological Society of America Bulletin,* **116**, 619-636, https://doi.org/10.1130/B25170.J

Daly, M.C., Lawrence, S.R., Kimun'a, D. and Binga, M. 1991. Late Paleozoic deformation in central Africa: a result of distant collision? *Nature,* 350, 605-607, https:// doi.org/ 10.1038/350605a0

Dalziel, I.W.D. 1997. Neoproterozoic;-.Paleozoic geography and tectonics: Review, hypothesis, environmental speculation. *Geological Society of America Bulletin,* **109**, 16--42, hnps://doi.org/l0.1130/0016-7606(l997)109<0016:ONPGAT>2.3.CO;2

Dalziel, I.W.D. and Elliot, D.H. 1982. West Antarctica: Problem child of Gondwanaland. *Tectonics,* **1**, 3--19, https:// doi.org/10.1029/TCOOJiOOI p00003

DeCelles, P.G., Gebrels, G.E., Quade, J., LaReau, B. and Spurlin, M. 2000.Tectonic implications ofU-Pb zircon agesof the Himalayan orogenic belt in Nepal. *Science,* **288,** 497-499, https://doi.org/ 10.1126/ science.288. 5465.497

de Wit,MJ. 1992.The CapeFold Belt: achallengeforanintegrated approach to inversion tectonics. *In:* de Wit, M.J. and Ransome, !.G.D. (eds) *Inversion Tectonics of the Cape Fold Bel Karooand Cretaceous Basinsof Southem Africa.* Balkema, Rotterdam,The Netherlands, 3--12.

de Wit, **M.J.**, Booth, P., Shone, R. and Bronn, P. 1998. *Cape Fold Belt Excursion Guide.* Gondwana 10 Post-Conference Field Trip P04, Cape Town, South Africa.

Dezes, P. 1999. *TectonicandMetamorphicEvolutionofthe Central Himalayan Domain in Southeast ZLlnskar, Kashmir, India.* PhD thesis, University of Lausanne, Lausanne, Switzerland.

Draganits, E., Grasemann, B. and Hager, C. 2005. Conjugate,cataclastic deformation bands in the Lower Devonian Muth Formation (Tethyan Zone, NW lndia): evidence for pre-Himalayan deformation structures. *Geological Magazine,* **142,** 765-781, https://doi.org/ I0.1017/S00l6756805001056

Duebendorfer, E.M. and Rees, M.N. 1998. Evidence for Cambrian deformation in the Ellsworth-Whitmore Mountains terrane, Antarctica: Stratigraphic and tectonic implications. *Geology,* **26,** 55-58, https://doi.org/10.1130/0091-7613(1998)026<0055:EFCDIT>2.3.CO;2

du Toit, A.L. 1937. *Our Wandering Continents.* Oliver and Boyd, Edinburgh, UK.

Elliot, R.A. 2013. The geological and tectonic evolution of the Transantarctic Mountains: a review. *Geological Society, London, Special Publications,* **381,** 7-35, https://doi.org/10.1144/SP381.14

Encamaci6n, **J.** and Grunow, A. 1996. Changing magmatic and tectonic styles along the paleo-Pacific margin of Gondwana and the onsetof early Paleozoic magmatism in Antarctica. *Tectonics,* **15,** 1325-1341, https://doi.org/l0.1029/96TC01484

Engelder, T. 1979. The **nalure** of deformation within the outerlimits of the central Appalachian fa-eland fold-and-lhrust belt in New York state. *Tectonophysics,* 55, 289-310, https://doi.org/10.1016/0040-1951(79)90181-1

Evans, M.A. and Dunne, W.M. 1991. Strain factorization and partitioning in the North Mountain thrust sheet, central Appalachians, USA *Journalof Structural Geology,* 13, 21-35, https://doi.org/l0.1016/0191-8141 (91)90098-4

Evans, **M.A.** and Groshong, R.H., JR 1994. A Computer program for the calcite strain-gauge technique. *Journal of Structural Geology,* **16,** 277-281, https://doi.org/ 10.1016/0191-8141(94)90110-4

Ferrill, D.A. 1991. Calcite twin widths and intensities as metamotphic indicators in natural low-temperature deformation of limestone. *Journal of Structural Geology,* **13,** 675--077, https://doi.org/10.1016/ 0191-8141(91)90029-I

Ferrill, **D.A** 1998. Critical re-evaluation of differential stress estimates from calcite twins in coarse-grained limestone. *Tectonophysics,* 285, 77--86, https://doi.org/10.1016/S0040-l951(97)00190-X

Ferrill, D.A, Morris, A., Evans, M.A., Burkhard, M., Groshong, R.H. and Onasdl, C.M. 2004. Calcite twin motphology: a low-temperature deformation geahermometer. *Journal of Structural Geology,* 26, 1521-1529, https://doi.org/l0.1016/j.jsg2003.11.028

Foden, **J**., Elburg, **M.A.,** Dougherty-Page, J. and Burtt, A. 2006.The timing and durationof the Delamerian Orogeny:correlation with the RossOrogen and implications for Gondwana assembly. *Journal of Geology,* **114,** 189-210, https://doi.org/10.1086/499570

Foster, D.A., Gray, D.R. and Spaggiari, C. 2005. Timing of subduction and exhumation along the Cambrian East Gondwana margin, and the formation of Paleozoic backarc basins. *Geological Society of America Bulletin,* **117,** 105-116, https://doi.org/10.1130/ B25481.1

Frakes, LA. andCrowell, J.C. 1967. Faciesand paleogeography of Late Paleozoic diamictite, Falkland Islands. *Geological Society of America Bulletin,* 78, 37-58, https:// doi.org/ 10.1130/0016-7606(1967)78[37:FAPOLP]2.0.CO;2

Frakes, L.A. and Crowell, J.C. 1969. Late Paleozoic glaciation; I, South America *Geological Society of America Bulletin,* 80, 1007-1041, hnps://doi.org/10.1130/ 0016-7606(1969)80[1007:LPGISA]2.0.CO;2

Frakes, L.A., Kemp, E.M. and Crowell, J.C. 1975. Late Paleozoic glaciation: part VI, Asia.*Geological Society of America Bulletin,* **86,** 454-464, https://doi.org/ 10. 1130/0016-7606(1975)86<454:LPGPVA>2.0.CO;2

Garcia-Arias,**M.,** Diez-Montes, **A.,** Villaseca, C. and Blanco-Quintero, I.F. 2018. The Cambro-Ordovician Olio de Sapo magmatism in the Iberian Massif and its Variscan evoluticn. *Earth-Science Reviews,* **176,** 345-372, https://doi.org/10.1016/j.earscirev.2017.11.004

Garzanti, E., Casnedi, R. and Jadoul, F. 1986. Sedimentary evidence of a Cambro-Ordovician orogenic event in the northwestern Himalaya. *Sedimentary Geology,* **48,** 237-265, https://doi.org/10.1016/0037-0738(86) 90032-1

Gehrels, G.E., DeCelles, P.G., Martin, A., Ojha, T.P., Pinhassi, G. and Upreti, B.N. 2003. Initiation of the Himalayan orogen as an early Paleozoic thin-skinned thrust belt. *GSA Today,* 13, 4-9, hnps://doi.org/10.1130/ I052-5173 (2003)I3<4:IOTHOA>2.0.CO;2

Gehrels, G.E., DeCelles, P.G., Ojha, T.P. and Upreti, B.N. 2006. Geologic and U-Th-Pbgeochronologicevidence for early Paleozoic tectonism in the Kathmandu thrust sheet, central Nepal Himalaya *Geological Society of America Bulletin,* **118,** 185-198, https://doi.org/ 10. 1130/B25753.1

Glen, R.A. 2005. The Tasmanides of eastern Australia *Geological Society, London, Special Publications,* **246,** 23--96, https://doi.org/10.1144/GSL.SP.2005. 246.01.02

Gonzalez, P.D., Sato, **A.M.** *et al.* 2018. Patagonia--Antarctica Early Paleozoic conjugate margins: Cambrian synsedimentary silicic magmatism, U-Pb dating of K-bentonites, and related volcanogenic rocks. *Gondwana Research,* 63, 186-225, https://doi.org/ 10. I016/j.gr.2018.05.0 IS

Goodge, J.W. 2020. Geological and tectonic evolution of the Transantarctic Mountains, from ancient craton to recent enigma *Gondwana Research,* **80,** 50--122, https://doi.org/10.1016/j.gr.2019.11.001

Goodge,J.W., Walker, N.W.and Hansen, V.L. 1993. Neoproterozoic--Carnbrian basement-involved orogenesis within the Antarctic marginofGondwana *Geology,* **21**, 37--40, https://doi.org/10.1130/0091-7613(1993) 021<0037:NCBIOW>2.3.CO;2

Goodge, J.W., Myrow, P., Phillips, D., Fanning, C.M. and Williams, l.S. *2004a.* Siliciclastic record of rapid denudation in response to convergent-margin orogenesis, Ross Orogen, Antarctica. *Geological Society of America Special Papers,* 378, 105-126, https://doi.org/10.1130/0-8137-2378-7.105

Goodge, J.W., Williams, LS. and Myrow, P. *2004b.* Provenance of Neoproterozoic and lower Paleozoic siliciclastic rocks of the central Ross orogen, Antarctica: detrital record of rift-, passive-, and active-margin sedimentation. *Geological Society of America Bulletin,* **116**, 1253-1279, https://doi.org/10.1130/B25347.1;16

Goodge, J.W., Fanning, C.M., Brecke, D.M., Licht, K.J. and Palmer, E.F. 2010. Continuation of the Laurentian Grenville Province across the Ross Sea Margin of East Antarctica. *Journal of Geology,* **118**, 601-619, https://doi.org/10.1086/656385

Gray, M.B., Starnatakos, J.A., Ferrill, D.A. and Evans, M.A. 2005. Fault-zone deformation in welded tuffs at Yucca Mountain, Nevada, USA. *Journal of Structural Geology,* 27, 1873-1891, https://doi.org/10.1016/j.jsg.2005.01.018

Groshong, **R.H., JR** 1972. Strain calculated from twinning in calcite. *Bulletin of the Geological Societyof America,* **83,** 2025-2038, https://doi.org/10.1130/0016-7606(1972)83[2025:SCFrlC]2.0.CO;2

Groshong, R.H., JR1974. Experimental testofleast-squares strain calculations using twinned calcite. *Bulletin of the Geological Societyof America,* 85, 1855-1864, https://doi.org/10.1130/0016-7606(1974)85< 1855:ErOLSG>2.0.CO;2

Groshong, R.H., JR 1975. Strain, fractures, and pressure solution in natural single-layer folds. *Bulletin of the Geological Society of America,* 86, 1363-1376, https:// doi.org/10.1130/0016-7606(1975)86<1363:SFAPSI>2.0.CO;2

Groshong, R.H.,JR1976. Strain and pressuresolution in the Martinsburg slate, Delaware Water Gap, New Jersey. *American Journal of Science,* 276, 1131-1146, https://doi.org/ 10.2475/ajs.276.9.1131

Groshong, R.H., JR, Teufel, L.W. and Gasteiger, C.M. 1984. Precision and accuracy of the calcite strain-gage technique. *Bulletin of the Geological Society of America,* 95, 357-363, https://doi.org/10.1130/0016-7606(1984)95<357:PAAOTC>2.0.CO;2

Hagen-Peter, G., Cottle, J.M., Smit, M. and Cooper, A.F. 2016. Coupled garnet Lu-Hf and monazite U-Pb geochronology constrain early convergent margin dynamics in the Ross orogen, Antarctica. *Journal of Metam()rphic Geology,* **34**, 293-319, https://doi.org/10.1111/jmg.12182

Halbich, I.W. 1992.Thecapefold beltorogeny: stateof the art 1970s-L980s. *In:*de Wit, M.J.and Ransome, I.G.D. (eds) *Inversion Tecwnics of the Cape Fold Belt, Karoo and Cretaceous Basins of Southern Africa.* Balkema, Rotterdam, The Netherlands, 141-158.

Halbich, I.W. and Swart, J. 1983. Structural zoning and dynamic history of the cover rocks of the Cape fold belt. *Geological Society of South Africa Special Publications,* **12,** 75-100.

Hayden, H.H. 1904. *The Geology of Spit with Parts of Bashahr and Rupshu.* Memoirs of the Geological Survey of India, 36.

Hughes, N.C., Myrow, P.M. *et al.* 2011. Cambrian rocks and fauna of the Wachi La, Black Mountains, Bhutan. *Geological Magazine,* **148**, 351-379, https://doi.org/10.1017/S0016756810000750

Isbell, J.L. 1999. The Kukri Erosion Surface; a reassessment of its relationship to rocks of the Beacon Supergroup in the central Transantarctic Mountains, Antarctica. *Antarctic Science,* **11**, 228-238, https://doi.org/10.1017/S0954102099000292

Johnson, **M.R.W.** 1994. Culminations and domal uplifts in the Himalaya *Tectonophysics,* 239, 139--147, https://doi.org/10.1016/0040-1951(94)90111-2

Johnston, S.T. 2000. The Cape Fold Belt and Syntaxis and the rotated Falklands Islands: dextral transpressional tectonics along the southwest margin of Gondwana *Journal of African Earth Sciences,* 31, 51-63, https://doi.org/ 10.1016/S0899-5362(00)00072-5

Kilsdonk, W. and Wiltschko, D.V. 1988. Deformation mechanisms in the southeastern ramp region of the Pine Mountain block, Tennessee. *Geological Society of America Bulletin,* **100**, 644-653, https://doi.org/I0.1130/0016-7606(1988) 100<0653:DMITSR>2.3.CO;2

Lacombe, O. and Laurent, P. 1996. Determinationofdeviatoric stress tensors based on inversion of calcite twin data from experimentally deformed monophase samples: preliminary results. *Tectonophysics,* 255, 189--202, https://doi.org/ 10.1016/0040-1951(95)00136-0

Lacombe, 0., Parlangeau, C., Beaudoin, N. and Amrouch, K. 2021,Calcite twin formation, measurement aduse as stress-strain indicators: a review of progress over the last decade. *Geosciences,* **11,** 445, https://doi.org/ 10.3390/geosciencesll 110445

Li, Z.X. and Powell, C.M. 2001. An outlineof the palaeogeographic evolution of the Australasian region since the beginning of the Neoproterozoic. *Earth-Science Reviews,* 53, 237-277, https://doi.org/10.1016/S0012-8252(00)00021-0

Loewy, S.L., Dalziel, l.W.D., Pisarevsky, S., Connelly, J.N., Tait, J., Hanson, R.E. and Bullen, D. 2011. Coats Land crustal block, East Antarctica: A tectonic tracer for Laurentia? *Geology,* 39, 859-862, https://doi.org/10.l130/G32029.1

Long, S., McQuarrie, N., Tobgay, T. and Grujic, D. 20I I. Geometry and crustal shortening of the Himalayan fold-thrust belt,eastern andcentral Bhutan. *Geological Society of America Bulletin,* **123,** 1427-1447, https://doi.org/10.1130/B30203.l

Malone, D.H., Stein, C.A., Craddock, J.P., Kley, J., Stein, S. and Malone, J.E. 2016. Maximum depositional age of the Neoproterozoic Jacobsville Sandstone, Michigan: implications for theevolution of the Midcontinent Rift. *Geosphere,* **12**, 1271-1282, https://doi.org/10.1130/GES0L302.1

Meert, J.G. 2003. A synopsis of events related to the assembly of eastern Gondwana. *Tecwnophysics,* 362, 1-40, https://doi.org/10.1016/S0040-1951(02)00629-7

Meert, J.G. and Powell, C.M. 2001. Assembly and break-up ofRodinia: introduction to thespecial volume. *Precambrian Research,* **110,** 1-8, https://doi.org/10.1016/S030L-9268(01)00177-2

Meert, J.G. and Torsvik, T.H. 2003. The making and unmakingof a supercontinent Rodinia revisited. *Tecto-ncphysics,* 375, 261-288, https://doi.org/10.1016/S0040-1951(03)00342-I

Millar, I.L. and Pankhurst, R.J. 1987. Rb-Sr geochronology of the region between the Antarctic Peninsula and the Transantarctic Mountains; Haag Nunataks and Mesozoic granitoids; Gondwana six; structure, tectonics, andgeophysics. *American Geophysical UnionGeophysical Moncgraph Series,* **40,** 151-160, https://doi.org/10.1029/GM040p0151

Millar, I.L. and Storey, B.C. 1995. Early Palaeozoic rather than Neoproterozoic volcanism and rifting within the Trans-Antarctic Mountains. *Journal of the Geological Society, London,* **152,** 417-420, https://doi.org/ 10.1144/gsjgs.152.3.0417

Miller, C., Tiioni, M., Frank, W., Grasemann, B., Klotzli, U., Guntli, P. and Draganits, E. 2001. Theearly Palaeozoic magmatic event in the Northwest Himalaya, India: source, tectonic setting and age of emplacemenL *Geological Magazine,* **138,** 237-251, https://doi.org/10.IOI7/S0016756801005283

Mosar, J. 1989. Internal deformation in the Prealpes Medianes, Switzerland. *Eclogae Geologicae Helvetiae,* 82, 765-793.

Millier, R.D., Cannon, J. *et al.* 2018. GPlates: Building a virtual Earth through deep time. *Geochemistry, Geophysics, Geosystems,* 19, 2243- 2261, https://doi.org/10.I029/2018GC007584

Myrow, P.M., Pope, M.C., Goodge, J.W., Fischer, W. and Palmer, A.R. 2002. Depositional history of pre-Devonian strata and timing of Ross orogenic tectonism in the central Transantarctic Mountains, Antarctica. *Geological Society of America Bulletin,* **114,** 1070-1088, https:// doi.org/10.1130/0016-7606(2002)114< 1070:DHOPDS>2.0.CO;2

Myrow, **P.M.,** Hughes, N.C. *et al.* 2003. Integrated Tectonostratigraphic reconstruction of the Himalaya and implications for its tectonic reconstruction. *Earth and Planetary Science letters,* **212,** 433-441, https://doi.org/10.1016/SOOl2-821X(03)00280-2

Myrow, P.W., Snell, K.E., Hughes, N.C., Paulsen, T.S., Heim, N.A. and Parcha, S.K. *2006a.* Cambrian depositional history of the Zanskar Valley region of theIndian Himalaya: tectonic implications. *Journal of Sedimentary Research,* 76, 364-381, https://doi.org/ 10.2110/jsr.2006.020

Myrow, P.W., Thompson, K.R., Hughes, N.C., Paulsen, T.S., Sell, B.K. and Parcha, S.K. 2006b. Cambrian stratigraphy and depositional history of the northern Indian Himalaya,Spiti Valley, north-central India. *Geological Society of America Bulletin,* **118,** 491-510, https://doi.org/lO.1130/B25828.I

Myrow, **P.M.,** Hughes, N.C., Searle, **M.P.,** Fanning, C.M., Peng, S.-C.and Parcha, S.K. 2009, Stratigraphic correlation of Cambrian-Ordovician deposits along the Himalaya: Implications for the age and nature of rocks in the Mount Everest region. *Geological Society of America Bulletin,* **120,** 323-332, https://doi.org/I0.1130/B26384.I

Myrow, P.M., Hughes, N.C., McKenzie, N.R., Pelgay, P., Toomson, T.J., Haddad, E.E. and **Mak** Fanning, C. 2016. Cambrian-Ordovician orogenesis in Himalayan equacrial Gondwana *Geologirol Society of America Bulletin,* **128,** 1679-1695, https://doi.c.rg/10.1130/B31507.I

Nelson, D.A. and Tuttle, J.M. 2018. The secular development of accretionary wedges: linking the Gondwana magmatic arc record of West Antarctica, Australia and South America. *Gondwana Research,* **63,** 15-33, https:// doi.org/ I0.1016/j.gr.2018.06.002

Nuriel, **P.,** Weinberger, R., Kylander-Clark, **A.R.C.,** Hacker, B.C. and Craddock, J.P. 2017. The onset of the Dead Seatransform based on calcite age-strain analyses. *Geology,* 45, 587-590, hnps:// doi.org/10.1130/038903.1

Nuriel, P., Craddock, J.P. *et al.* 2019. Reactivation history of the Bolu-Oerede segment of the North Anatolian Fault Zone based on calcite age-strain analyses. *Geology,* **47,** 465-467, https://doi.org/l0.1130/G45727.I

Owens, W.H. 1984. Thecalculation of the best-fit ellipsoid from elliptical sections on atbitrarily oriented planes. *Journal of Structural Geology,* 6, 571-578, https:/ / doi.org/ I0.1016/0191-8141(84)90066-X

Palin, R.W., Treloar, P.J., Searle, M.P., Wald, T., White, R.W. and Mertz-Kraus, R. 2018. U-Pb monazite ages from the Pakistan Himalaya record pre-Himalayan Ordovician orogeny and Permian continental breakup. *GSA Bulletin,* **130,** 2047-2061, https://doi.org/10.I130/B31943.1

Pas, D., DaSilva, A, Dhital,M.R andBoulvain,F. 201I.Sedimentology of a Mid-Late Ordovician carbonate mud-mound complex from the Kathmandu nappe in Central Nepal. *Journal of Asian Earth Sciences,* 42, 452-467, https://doi.org/l0.I016/j.jseais2011.05.008

Paulsen, T.S., Encarnacion, J. andGrunow, **A.M.** 2004. Structure and timing of transpressional deformation in the Shackleton Glacier area, Ross orogen, Antarctica. *Journal of the Geological Society, London,* **161,** 1027-1038, https://doi.org/l0.1144/0016-764903-040

Paulsen, T.S., Demosthenous, C.M., Myrow, P.M., Hughes, N.C. and Parcha, **S.K.** 2007a. Paleostrain stratigraphic analysis of calcite twins across the Cambrian-Ordovician unconformity in the Tethyan Himalaya, Spiti and Zanskar valley regions, India *Journal of Asian Earth Sciences,* **31,** 44-54, https://doi.org/I0.1016/j.jseaes.2007.04.00I

Paulsen, T.S., Encarnacion, **J.,** Grunow, A.M., Layer, P.W. and Watkeys, M. 2007b. New age constraints for a short pulse in Ross orogen deformation triggered by East-West Gondwana suturing. *Gondwana Research,* 12, 417-427, https://doi.org/10.1016/j.gr.2007.05.011

Paulsen, T.S., Encarnacion, J., Grunow, A., Valencia, V.A. and Rasoazanamparany, C. 2008. Late sinistral shearing along Gondwana's paleo-Pacific margin in the Ross orogen, Antarctica: New structure and age data from the O'Brien Peak area. *The Journal of Geology,* **116,** 303-312, https://doi.org/ 10.1086/587727

Paulsen, T.S., Wilson, T.J., Dernosthenous, C., Millan, C., Jarrad, R. and Laufer, A. 2014. Kinematics of the Neogene Terror rift:constraints from calcite twinning strains in the ANDRILL McMurdo Ice Shelf (AND-IB) core, Victoria Land Basin, Antarctica. *Geosphero,* 10, 82&-841, https://doi.org/10.1130/GES01002.I

Paulsen, T.S., Encarnacion, J., Grunow, A.M., Stump, E., Pecha, M. and Valencia, V.A. 2018. Correlation and late-stage deformation of Liv Group volcanics in the

Ross-Delamerian orogen, Anlarctica, from new U-Pb ages. *The Journal of Geology,* **126**, 307-323, https://doi.org/10.1086/ 697036

Paulsen, T.S., Encarnacion, J., Grunow, **A.M.**, Valencia, **V.A.**, Pecha, **M.A.**, Benowitz, **J.** and Layer, **P.** 2021. New ages from the Shackleton Glacier area and their context in the regional tectonomagmatic evolution of the Ross orogen of Antarctica. *International Geology Review,* 63, 1596--1618, https://doi.org/10.1080/00206814.2020.1786737

Powell, C.M., Li, Z.X., McElhinny, **M.W.**, Meert, J.G. and Park,J.K. 1993. Paleomagnetic constraintson timingof the Neoproterozoic breakup of Rodinia and the Cambrian formation of Gondwana. *Geology,* **21**, 889-892, https://doi.org/10.1130/0091-7613(1993)021<0889:PCOTOT>2.3.CO;2

Ramos, V.A. 1988a. The tectonics of the Central Andes: 30° to 35° S latirude. *Geological Society of America Special Papers,* 218, 31-54, https://doi.org/10.1130/SPE218-p31

Ramos, V.A. 1988b. Tectonics of the Late Proterozoic--Early Paleozoic: a collision history of southern South America. *Episodes,* 11, 168-174, https://doi.org/10.18814/epiiugs/ 1988/vl li3/003

Rowe, K.J. and Rutter, E.H. 1990. Paleostress estimation using calcite twinning: experimental calibration and application to narure. *Journal of Structural Geology,* 12, 1-17, https://doi.org/10.1016/0191-8141(90)90044-Y

Schmitt, R.S., Trouw, R.A.J., Van Schmus, W.R. and Pimentel, **M.M.** 2004.Late amalgamation in the central part of West Gondwana: new geochronological data and thecharacterizationof a Cambrian collisional orogeny in the Ribeira Belt (SE Brazil). *Precambrian Research,* 133, 29-61, https://doi.org/10.1016/j.precarnres.2004.03.010

Schmitt, R.S., Trouw, R.A.J., Van Schmus, W.R. and Passchier, C.W. 2008.Cambrian orogeny in the Ribeira Belt (SE Brazil) and correlations within West Gondwana: ties that bind underwater. *Geological Society, Lendon, Special Publications,* 294, 279-296, https://doi.org/10.1 144/SP294.15

Schmitt, R.S., Trouw, R.A.J., Passchier, C.W., Medeiros, S.R. and Armstrong, R.A. 2012. 530 Ma syntectonic syenites and granites in NW Namibia - their relation with collision along the junction of the Damara and Kaoko belts. *Gondwana Research,* **21**, 362-377, https://doi.org/10.1016/j.gr.2011.08.006

Schmitt, R.S., de Fragoso, R.A. and Collins, A.S. 2018. Suturing Gondwana in the Cambrian: the orogenic events of the final amalgamation. *In:* Siegesmund, S., Basei, M.A.S., Oyhant9abal, P. and Oriolo, S. (eds) *Geology of Southwest Gondwana.* Springer, Cham, Switzerland, 411-432, https://doi.org/ IQ.I 007 /978-3-319-68920-3_15

Spang, J.H. and Groshong, R.H., JR 1981. Deformation mechanisms and strain history of a minor fold from the Appalachian Valley and Ridge Province. *Tectonophysics,* 72, 323-342, https://doi.org/10.1016/0040-1951(81)90244-4

Sporli, K.B. andCraddock, C. 1992. Strucrure of the Heritage Range, Ellsworth Mountains, West Antarctica; geology and paleontology of the Ellsworth Mountains, West Antarctica. *Geological Society of America Memoirs,* **170**, 375-392, https://doi.org/10.1130/MEM170-p375

Storey, B.C., Macdonald, D.I.M., Dalziel, I.W.D., Isbell, J.L. and Millar, I.L. 1996. Early Paleozoic sedimentation, magmatism, and deformation in the Pensacola Mountains, Antarctica: the significance of the Ross orogeny. *Geological Society of America Bulletin,* **108**, 685-707, https://doi.org/10.1130/0016-7606(1996)108<0685:EPSMAD>2.3.CO;2

Srump, E. 1982. The Ross Supergroup in the Queen Maud Mountains. *In:*Craidock, C. (ed.) *Antarctic Geoscience.* University of Wisconsin Press, Madison, WI, 565-569.

Stump, E. 1986. Stratigraphy of the Ross Supergroup, Central Transantarctic Mountains. *American Geophysical Union Antarctic Research Series,* 36, 225-274, https:// doi.org/10.1029/ AR036p0225

Stump, E. 1992. The Ross orogen of the Transanlarctic Mountains in light of the Laurentia-Gondwana split *GSA Today,* 2, 25-31.

Srump, E. 1995. *The Ross Orogen of the Transantarctic Mountains.* Cambridge University Press, Cambridge, **UK.**

Teufel, L.W. 1980. Strain analysis of experimental superposed deformation using calcite twin lamellae. *Tectonophysics,* 65, 291-309, https://doi.org/10.1016/0040-1951(80)90079-7

Tohver, E., D' Agrella Filho, M. and Trindade, **R.I.F.** 2006. Paleomagnetic record of Africa and South America for the 1200-500 Ma interval, and evaluation of Rodinia and Gondwana assemblies. *Precambrian Research,* **147**, 193-222, https://doi.org/10.1016/j.precarnres.2006.01.015

Torsvik, T.H.2003. TheRodiniajigsaw puzzle. *Science,* **300**, 1379-1381, https://doi.org/10.1126/science.1083469

Torsvik, T.H. and Robin Cocks, L. 2013. Gondwana from top to base in space and time. *Gondwana Research,* **24**, 999-1030, https://doi.org/10.1016/j.gr.2013.06.012

Torsvik, T.H., Paulsen, T.S., Hughes, N.C., Myrow, **P.M.** and Ganerod, **M.** 2009. The Tethyan Himalaya: palaeogeographical and tectonic constraints from Ordovician palaeomagneticdata.*Journalof the Geological Society, Lendon,* **166**, 679-687, https://doi.org/10.1144/0016-76492008-123

Turner, F.J. 1953. Narure and dynamic intetpretation of deformation lamellae in calcite of three marbles. *American Journal of Science,* **251**, 276-298, https://doi.org/ 10.2475/ ajs.251.4.276

Turner, F.J. 1962. Compression and tension axes deduced from (0112) Twinning in Calcite. *Journal of Geophysical Research, 61,* 1660.

Veevers, J.J., Walter, M.R. and Scheibner, E. 1997. Neoproterozoic tectonics of Australia-Anlarctica and Laurentia and the 560 Ma birth of the Pacific Ocean reflect 400 m.y. Pangean supercycle. *Journal of Geology,* 105, 225-242, https://doi.org/10.1086/515914

Vieira, T.A., Schmitt, R.S. *et al.* 2022. Contrasting *P-T-l* paths of basement and cover within the Buzios orogen, SE Brazil - tracking Ediacaran-Cambrian subduction zones. *Precambrian Research,* **368**, 106479, https://doi.org/ 10.1016 /j.precamres.2021.106479

Villaseca, C., Merino Martfnez, E., Orejana, D., Andersen, T. and Belousova, E. 2016. Zircon Hf signarures from granitic orthogneisses of the Spanish Central System: Significance and sources of the Cambro-Ordovician magmatism in the Iberian Variscan Belt. *Gondwana Research,* **34**, 60-83, https://doi.org/ LO.I 016/j.gr.2016.03.004

von Gosen, W., Buggisch, W. and Krumm, S. 1991. Metamorphism and deformation mechanisms in the Sierras Australes told and thrust belt (Buenos Aires province, Argentina). *Tecronophysics,* **185**, 335-356, https://doi.org/ 10.1016/0040-1951(91)90453- Y

Wang, Y., Li, Q. and **Qu,** G. 2006. ^{40}Ar/3^{9}Arthermochronological constraints on the cooling and exhumation history of the South Tibetan Detachment System, Nyalam area, southern **Tibet.** *Geological Society, London, Special Publications,* **268,** 327-354, https://doi.org/L0.1144/GSL.SP.2006.268.01.16

Wang, Y., Li, Q. and Qu, G. 2015. Timing of partial melting and cooling across the Greater Himalayan Crystalline Complex (Nyalam, Central Himalaya): in-sequence thrusting and its implications. *Journal of Petrology,* 56, 1677-1702, https://doi.org/10.1093/petrology/egv050

Webers, G.F., Bauer, R.L., Anderson, J.M., Buggisch, W., Ojakangas, R.W. and Sporli, K.B. 1992. The Heritage Group of the Ellsworth Mountains, West Antarctica; geology and paleontology of the Ellsworth Mountains, West Antarctica *Geological Society of America Memoirs,* 170, 9-19, https://doi.org/10.1130/MEMI70-p9

Weinberger, R., Nuriel, P., Kylander-Clark, A.R.C. and Craddock, J. 2020. Temporal and spatial relations between large-scale fault systems: evidence from the Sinai-Negev shear zone and the Dead Sea Fault. *Earth-Science Reviews,* **211,** L03377, https://doi.org/ LO.I016/j.earscirev.2020.L03377

Wenk, H.-R., Takeshita, T., Bechler, E., Erskine, B.G. and Matthies, S. I987. Pure shear and simple shear calcite textures. Comparison of experimental, theoretical and natural data *Journal of Stmctural Geology,* 9, 731-745, https://doi.org/L0.1016/0191-8141(87)90156-8

Wiesmayr, G. and Grasemann, B. 2002. Eohimalayan fold and thrust belt implications for the geodynamic evolution of the NW-Himalaya, lndia. *Tecronics,* 21, 1-18, https:// doi.org/ IO.L029/2002TCOOl 363

Wilson, J.T. 1966. Did the Atlantic close and then reopen? *Nature,* 211, 676-681, https://doi.org/10.L038/211676a0

Wiltschko, D.V., Medwedeff, D.A. and Millson, H.E. 1985. Distribution and mechanisms of strain within rocks on the northwest ramp of Pine Mountain block, southern Appalachian foreland: a field test of theory. *Geological Society of America Bulletin,* 96, 426-435, https://doi.org/10.1130/0016-7606(1985)96<426:DAMOSW>2.0.CO;2